nuclei in the cerebral pia mater along the basal lamina, but did not find many β-gal-positive nuclei in the cerebellum. There are several possibilities to explain this discrepancy. The first possibility is that the domain that regulates utrophin expression in the pia mater of the cerebellum is different from that for the pia mater in the cerebrum. The second possibility is that transcription of utrophin might be less active in fibroblastic cells of the pia mater of cerebellum compared to those in the cerebrum. However, a fundamental difference between fibroblastic cells in the cerebrum and those in the cerebellum has not been reported; further experiments are required to explain this discrepancy.

We demonstrated that DUE is necessary for utrophin expression in skeletal muscle, but the increase in the utrophin expression level was much larger than the transgene expression in regenerated muscle. Another study [11] also detected the increase in the abundance of A-utrophin protein in muscle from *mdx* mice but could not find any parallel elevation in the levels of utrophin transcripts. Therefore, A-utrophin expression may also be regulated at the post-transcriptional level. Indeed, recent studies have shown that distinct cis-acting elements within the utrophin 3′-UTR were important not only for controlling the stability of utrophin transcripts in muscle cells, but also for targeting them to specific subcellular locations [34,35].

Post-translational levels are also important for utrophin expression through stabilization of the protein. DAPs such as dystrophin, β-dystroglycan, α-dystroglycan, and α-sarcoglycan have been linked to regulation by protein degradation mechanisms including the ubiquitin-proteasome pathway [36] and calpain-mediated proteolysis [37]. Inhibition of the proteasomal degradation pathway was found to rescue the expression levels of several DAPs in *mdx* mice [36]. Treatment of normal and DMD human myotubes with glucocorticoid induced utrophin protein without elevations in transcripts, and this was suggested to involve calpain inhibition [38].

It is likely that extrasynaptic expression of utrophin in skeletal muscle of DMD patients would ameliorate the dystrophic pathology, at least to some extent [17,18]. The results of the present study demonstrate that DUE is indispensable to utrophin expression in skeletal muscle and heart. To further investigate the up-regulation mechanisms of utrophin in both tissues, we need to search for transcription factors bound to DUE. In addition, we established primary myogenic cell cultures from DUE Tg mice and found that utrophin up-regulation depends on the DUE motif during muscle differentiation. These cells provide a high through-put screening system for drugs that can up-regulate utrophin expression in myogenic cells.

Acknowledgements

We thank Dr Imamura for giving the utrophin antibody. We also thank all members of the Department of Molecular Therapy, National Institute of Neuroscience, for technical assistance and useful discussion and suggestions, especially S. Fukada, A. Uezumi, and M. Ikemoto. This work is supported by grants for Research on Nervous and Mental Disorders (grant 16B-2); Health Science Research Grants for research on the human genome and gene therapy (H16-genome-003) and for research on brain science (H15-kokoro-021 and H18-kokoro-019) from the Japanese Ministry of Health, Labour, and Welfare; Grants-in-Aid for Scientific Research (14657158, 15390281, 16590333, 17590857, and 18590392) from the Japanese Ministry of Education, Culture, Sports, Science, and Technology; and the Ground-based Research Program for Space Utilization, promoted by Japan Space Forum.

References

1. Koenig M, Hoffman EP, Bertelson CJ, *et al.* Complete cloning of the Duchenne muscular dystrophy (DMD) cDNA and preliminary genomic organization of the DMD gene in normal and affected individuals. *Cell* 1987; **50**: 509–517.
2. Ahn AH, Kunkel LM. The structural and functional diversity of dystrophin. *Nat Genet* 1993; **3**: 283–291.
3. Tinsley JM, Blake DJ, Zuellig RA, *et al.* Increasing complexity of the dystrophin-associated protein complex. *Proc Natl Acad Sci USA* 1994; **91**: 8307–8313.
4. Campbell KP. Three muscular dystrophies: loss of cytoskeleton-extracellular matrix linkage. *Cell* 1995; **80**: 675–679.
5. Ozawa E, Yoshida M, Suzuki A, *et al.* Dystrophin-associated proteins in muscular dystrophy. *Hum Mol Genet* 1995; **4**: 1711–1716.
6. Pearce M, Blake DJ, Tinsley JM, *et al.* The utrophin and dystrophin genes share similarities in genomic structure. *Hum Mol Genet* 1993; **2**: 1765–1772.
7. Grady RM, Teng H, Nichol MC, *et al.* Skeletal and cardiac myopathies in mice lacking utrophin and dystrophin: a model for Duchenne muscular dystrophy. *Cell* 1997; **90**: 729–738.
8. Khurana TS, Watkins SC, Chafey P, *et al.* Immunolocalization and developmental expression of dystrophin related protein in skeletal muscle. *Neuromuscul Disord* 1991; **1**: 185–194.
9. Ohlendieck K, Ervasti JM, Matsumura K, *et al.* Dystrophin-related protein is localized to neuromuscular junctions of adult skeletal muscle. *Neuron* 1991; **7**: 499–508.
10. Galvagni F, Cantini M, Oliviero S. The utrophin gene is transcriptionally up-regulated in regenerating muscle. *J Biol Chem* 2002; **277**: 19106–19113.
11. Weir AP, Burton EA, Harrod G, *et al.* A- and B-utrophin have different expression patterns and are differentially up-regulated in mdx muscle. *J Biol Chem* 2002; **277**: 45285–45290.
12. Takemitsu M, Ishiura S, Koga R, *et al.* Dystrophin-related protein in the fetal and denervated skeletal muscles of normal and mdx mice. *Biochem Biophys Res Commun* 1991; **180**: 1179–1186.
13. Matsumura K, Ervasti JM, Ohlendieck K, *et al.* Association of dystrophin-related protein with dystrophin-associated proteins in mdx mouse muscle. *Nature* 1992; **360**: 588–591.
14. Helliwell TR, Man NT, Morris GE, *et al.* The dystrophin-related protein, utrophin, is expressed on the sarcolemma of regenerating human skeletal muscle fibres in dystrophies and inflammatory myopathies. *Neuromuscul Disord* 1992; **2**: 177–184.
15. Nguyen TM, Ellis JM, Love DR, *et al.* Localization of the DMDL gene-encoded dystrophin-related protein using a panel of 19 monoclonal antibodies: presence at neuromuscular junctions, in the sarcolemma of dystrophic skeletal muscle, in vascular and other smooth muscles, and in proliferating brain cell lines. *J Cell Biol* 1991; **115**: 1695–1700.
16. Tinsley JM, Potter AC, Phelps SR, *et al.* Amelioration of the dystrophic phenotype of mdx mice using a truncated utrophin transgene. *Nature* 1996; **384**: 349–353.
17. Deconinck N, Tinsley J, De Backer F, *et al.* Expression of truncated utrophin leads to major functional improvements in dystrophin-deficient muscles of mice. *Nat Med* 1997; **3**: 1216–1221.

18. Tinsley J, Deconinck N, Fisher R, *et al*. Expression of full-length utrophin prevents muscular dystrophy in mdx mice. *Nat Med* 1998; **4**: 1441–1444.
19. Gilbert R, Nalbantoglu J, Petrof BJ, *et al*. Adenovirus-mediated utrophin gene transfer mitigates the dystrophic phenotype of mdx mouse muscles. *Hum Gene Ther* 1999; **10**: 1299–1310.
20. Yamamoto K, Yuasa K, Miyagoe Y, *et al*. Immune response to adenovirus-delivered antigens upregulates utrophin and results in mitigation of muscle pathology in mdx mice. *Hum Gene Ther* 2000; **11**: 669–680.
21. Dennis CL, Tinsley JM, Deconinck AE, *et al*. Molecular and functional analysis of the utrophin promoter. *Nucleic Acids Res* 1996; **24**: 1646–1652.
22. Burton EA, Tinsley JM, Holzfeind PJ, *et al*. A second promoter provides an alternative target for therapeutic up-regulation of utrophin in Duchenne muscular dystrophy. *Proc Natl Acad Sci USA* 1999; **96**: 14025–14030.
23. Jimenez-Mallebrera C, Davies K, Putt W, *et al*. A study of short utrophin isoforms in mice deficient for full-length utrophin. *Mamm Genome* 2003; **14**: 47–60.
24. Takahashi J, Itoh Y, Fujimori K, *et al*. The utrophin promoter A drives high expression of the transgenic LacZ gene in liver, testis, colon, submandibular gland, and small intestine. *J Gene Med* 2005; **7**: 237–248.
25. Hirst RC, McCullagh KJ, Davies KE. Utrophin upregulation in Duchenne muscular dystrophy. *Acta Myol* 2005; **24**: 209–216.
26. Galvagni F, Oliviero S. Utrophin transcription is activated by an intronic enhancer. *J Biol Chem* 2000; **275**: 3168–3172.
27. Kalderon D, Roberts BL, Richardson WD, *et al*. A short amino acid sequence able to specify nuclear location. *Cell* 1984; **39**: 499–509.
28. Ishii A, Hagiwara Y, Saito Y, *et al*. Effective adenovirus-mediated gene expression in adult murine skeletal muscle. *Muscle Nerve* 1999; **22**: 592–599.
29. Imamura M, Ozawa E. Differential expression of dystrophin isoforms and utrophin during dibutyryl-cAMP-induced morphological differentiation of rat brain astrocytes. *Proc Natl Acad Sci USA* 1998; **95**: 6139–6144.
30. Couteaux R, Mira JC, d'Albis A. Regeneration of muscles after cardiotoxin injury. I. Cytological aspects. *Biol Cell* 1988; **62**: 171–182.
31. Rando TA, Blau HM. Primary mouse myoblast purification, characterization, and transplantation for cell-mediated gene therapy. *J Cell Biol* 1994; **125**: 1275–1287.
32. Uezumi A, Ojima K, Fukada S, *et al*. Functional heterogeneity of side population cells in skeletal muscle. *Biochem Biophys Res Commun* 2006; **341**: 864–873.
33. Coso OA, Montaner S, Fromm C, *et al*. Signaling from G protein-coupled receptors to the c-jun promoter involves the MEF2 transcription factor. Evidence for a novel c-jun amino-terminal kinase-independent pathway. *J Biol Chem* 1997; **272**: 20691–20697.
34. Gramolini AO, Belanger G, Jasmin BJ. Distinct regions in the 3′ untranslated region are responsible for targeting and stabilizing utrophin transcripts in skeletal muscle cells. *J Cell Biol* 2001; **154**: 1173–1183.
35. Miura P, Thompson J, Chakkalakal JV, *et al*. The utrophin A 5′-untranslated region confers internal ribosome entry site-mediated translational control during regeneration of skeletal muscle fibers. *J Biol Chem* 2005; **280**: 32997–33005.
36. Bonuccelli G, Sotgia F, Schubert W, *et al*. Proteasome inhibitor (MG-132) treatment of mdx mice rescues the expression and membrane localization of dystrophin and dystrophin-associated proteins. *Am J Pathol* 2003; **163**: 1663–1675.
37. Lescop C, Herzner H, Siendt H, *et al*. Novel cell-penetrating alpha-keto-amide calpain inhibitors as potential treatment for muscular dystrophy. *Bioorg Med Chem Lett* 2005; **15**: 5176–5181.
38. Courdier-Fruh I, Barman L, Briguet A, *et al*. Glucocorticoid-mediated regulation of utrophin levels in human muscle fibers. *Neuromuscul Disord* 2002; **12**: S95–104.

HUMAN GENE THERAPY 19:719–730 (July 2008)

DOI: 10.1089/hum.2007.184

Recombinant Adeno-Associated Virus Type 8-Mediated Extensive Therapeutic Gene Delivery into Skeletal Muscle of α-Sarcoglycan-Deficient Mice

Akiyo Nishiyama,[1] Beryl Nyamekye Ampong,[1] Sachiko Ohshima,[1] Jin-Hong Shin,[1] Hiroyuki Nakai,[2] Michihiro Imamura,[1] Yuko Miyagoe-Suzuki,[1] Takashi Okada,[1] and Shin'ichi Takeda[1]

Abstract

Autosomal recessive limb-girdle muscular dystrophy type 2D (LGMD 2D) is caused by mutations in the α-sarcoglycan gene (α-SG). The absence of α-SG results in the loss of the SG complex at the sarcolemma and compromises the integrity of the sarcolemma. To establish a method for recombinant adeno-associated virus (rAAV)-mediated α-SG gene therapy into α-SG-deficient muscle, we constructed rAAV serotypes 2 and 8 expressing the human α-SG gene under the control of the ubiquitous cytomegalovirus promoter (rAAV2-α-SG and rAAV8-α-SG). We compared the transduction profiles and evaluated the therapeutic effects of a single intramuscular injection of rAAVs into α-SG-deficient ($Sgca^{-/-}$) mice. Four weeks after rAAV2 injection into the tibialis anterior (TA) muscle of 10-day-old $Sgca^{-/-}$ mice, transduction of the α-SG gene was localized to a limited area of the TA muscle. On the other hand, rAAV8-mediated α-SG expression was widely distributed in the hind limb muscle, and persisted for 7 months without inducing cytotoxic and immunological reactions, with a reversal of the muscle pathology and improvement in the contractile force of the $Sgca^{-/-}$ muscle. This extensive rAAV8-mediated α-SG transduction in LGMD 2D model animals paves the way for future clinical application.

Introduction

LIMB-GIRDLE MUSCULAR DYSTROPHY TYPE 2D (LGMD 2D) is caused by mutations in the α-sarcoglycan (α-SG) gene, and is the most frequent cause of the autosomal recessive LGMD. LGMD 2D patients have the clinical characteristics of progressive muscle necrosis in the proximal limb muscles (Eymard *et al.*, 1997). Sarcoglycans (SGs) are essential constituents of the dystrophin-associated protein (DAP) complex, which consists of several membrane-spanning and cytoplasmic proteins, including dystroglycans (α and β), SGs (α, β, γ, and δ), sarcospan, syntrophins (α_1, β_1, and β_2), and dystrobrevins that directly or indirectly associate with dystrophin (Ervasti *et al.*, 1990; Yoshida and Ozawa, 1990; Iwata *et al.*, 1993). A defect in any one of the four SGs can disrupt the entire SG complex. Mutations in four genes encoding α-, β-, γ-, and δ-SG are responsible for autosomal recessive LGMD 2D, 2E, 2C and 2F, respectively (Ervasti *et al.*, 1990; Bonnemann *et al.*, 1995; Noguchi *et al.*, 1995; Nigro *et al.*, 1996; Eymard *et al.*, 1997; Fanin *et al.*, 1997).

Many *in vivo* studies have demonstrated that recombinant adeno-associated virus (rAAV) packaged in various serotypes of AAV capsids exhibits serotype-specific tissue or cell tropism with different transduction efficiencies (Fisher *et al.*, 1997; Greelish *et al.*, 1999; Gao *et al.*, 2002, 2004; Wang *et al.*, 2005). rAAV has been shown to mediate long-term transgene expression in many tissues without evoking severe immune reactions. Some rAAVs efficiently transduce skeletal muscle (Kessler *et al.*, 1996; Xiao *et al.*, 1996; Fisher *et al.*, 1997). rAAV serotype 2 (rAAV2)-mediated muscle gene therapy is a promising approach, but it is effective only locally. In contrast, rAAV serotype 8 (rAAV8)-mediated gene transfer is capable of crossing capillary blood vessels to achieve systemic gene delivery, and effectively transduces genes into cardiac and skeletal muscle (Wang *et al.*, 2005). Therefore, rAAV8 is a good candidate for a therapeutic tool.

To assess the efficacy and therapeutic potential of rAAV8 for LGMD 2D, we directly injected rAAV2-α-SG and rAAV8-α-SG into the tibialis anterior (TA) muscles of 10-day-old α-SG-deficient mice (neonatal $Sgca^{-/-}$ mice). Our data suggested not

[1]Department of Molecular Therapy, National Institute of Neuroscience, National Center of Neurology and Psychiatry, Tokyo 187-8502, Japan.
[2]Department of Molecular Genetics and Biochemistry, University of Pittsburgh School of Medicine, Pittsburgh, PA 15261.

only the extensive expression of α-SG in Sgca$^{-/-}$ skeletal muscle, but also a robust level of expression of α-SG at the sarcolemma after a single intramuscular injection of rAAV8-α-SG. In addition, rAAV8-α-SG effectively transduced the cardiac muscle of 7-week-old Sgca$^{-/-}$ mice (adult Sgca$^{-/-}$ mice). Most importantly, 7 months after the injection of rAAV8-α-SG into neonatal Sgca$^{-/-}$ mice, expression of α-SG and improvement of sarcolemmal function were sustained, without inducing cytotoxic and immunological reactions. Thus, the AAV8 vector is a promising tool for gene therapy of LGMD 2D.

Materials and Methods

Recombinant AAV production

The full-length human α-SG cDNA was amplified from a skeletal muscle single-strand cDNA library (Human Skeletal Muscle Marathon-Ready cDNA; Clontech, Palo Alto, CA) by polymerase chain reaction (PCR) with the following set of oligonucleotide primers: 5′-CTCTGTCACTCACCGGG-3′ (nucleotide positions 2–18) and 5′-AGGATGAAGTC-AGGGCTGGAC-3′ (nucleotide positions 1223–1243) (McNally *et al.*, 1994). The amplification was carried out with LA-Taq polymerase (TaKaRa Bio, Shiga, Japan) for 30 cycles, with each cycle consisting of 94°C for 30 sec and 60°C for 2 min. The PCR products were then cloned into a TA cloning vector (Invitrogen, Carlsbad, CA), and sequenced with an ABI310 sequencer (Applied Biosystems, Foster City, CA). α-SG cDNA was then cloned into an AAV serotype 2 vector plasmid (Xiao *et al.*, 1998; Yuasa *et al.*, 2002) including the cytomegalovirus (CMV) promoter, splicing donor/acceptor (SD/SA) sites derived from the simian virus 40 (SV40), an SV40 poly(A) signal, inverted terminal repeat (ITR) of the AAV2 viral genome, and 2.0 kb of λ DNA, which served as a stuffer (depicted in Fig. 1A).

The vector genome was packaged in the AAV2 capsid or pseudotyped into the AAV8 capsid by triple transfection of

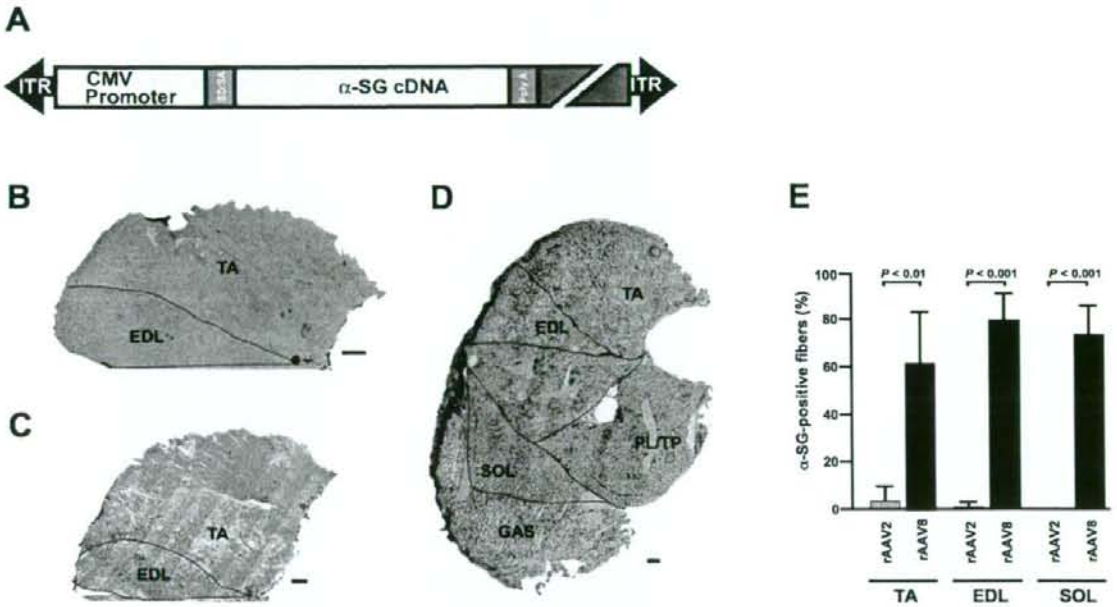

FIG. 1. Widespread expression of α-SG in hind limb muscles after a single injection of rAAV2-α-SG or rAAV8-α-SG into the tibialis anterior (TA) muscles of 10-day-old α-SG-deficient mice. (**A**) Genomic structure of rAAV used in this study. Human α-SG cDNA (1.2 kb) was inserted downstream of the CMV promoter. ITR, inverted terminal repeat from AAV2 genome; SD/SA, splicing donor/acceptor sites derived from SV40 intron; poly(A), a polyadenylation signal from SV40. The large shaded box represents a stuffer sequence derived from λ DNA. (**B–D**) Right TA muscles of neonatal Sgca$^{-/-}$ mice were injected with 1×10^{11} VG of rAAV2-α-SG (**C**) or rAAV8-α-SG (**D**). Four weeks after rAAV injection, the hind limb muscles of Sgca$^{-/-}$ mice were immunolabeled with a rabbit polyclonal antibody to α-SG. Hind limb muscles included the TA, extensor digitorum longus (EDL), plantaris (PL)/tibialis posterior (TP), soleus (SOL), and gastrocnemius (GAS) muscles. The TA and EDL muscles of Sgca$^{-/-}$ mice are shown as negative controls (**B**). Note that α-SG is expressed not only in rAAV8-injected TA muscle, but also in all hind limb muscles after direct injection of rAAV8-α-SG into the right TA muscle (**D**). Scale bars (**B–D**): 500 μm. (**E**) Percentages of α-SG-positive myofibers in TA, EDL, and SOL muscles after injection of rAAV2-α-SG (shaded columns) and rAAV8-α-SG (solid columns) injection into TA muscles of Sgca$^{-/-}$ mice. The right TA muscles of neonatal Sgca$^{-/-}$ mice were transduced with 1×10^{11} VG of rAAV2-α-SG or rAAV8-α-SG. Four weeks after rAAV injection, the hind limb muscles of Sgca$^{-/-}$ mice were immunolabeled with the α-SG antibody and then counterstained with hematoxylin and eosin. Hind limb muscles include the TA, EDL, and SOL muscles. The percentage of α-SG-positive myofibers was calculated on the basis of more than 200 total myofibers in cross-sections from three animals for each group. p Values are indicated and show statistical significance between Sgca$^{-/-}$ mice and rAAV8-injected Sgca$^{-/-}$ mice ($p < 0.01$ for TA, $p < 0.001$ for EDL, and $p < 0.001$ for SOL).

the AAV vector plasmid, AAV helper plasmid (p5E18-VD2/8) (Wang *et al.*, 2005), and adenovirus helper plasmid (XX6) (Xiao *et al.*, 1998) at a molecular ratio of 1:1:1 in 293 cells, using the calcium phosphate coprecipitation method (Wigler *et al.*, 1980). All the vectors were then purified by two cycles of cesium chloride gradient centrifugation, and concentrated as described by Burton and coworkers (1999). The final viral preparations were kept in phosphate-buffered saline. Physical particle titers were determined by a quantitative dot-blot assay.

Administration of rAAV vectors to murine skeletal muscle

All animal-handling procedures were done in accordance with a protocol approved by the committee of the National Institute of Neuroscience (National Center of Neurology and Psychiatry, Kodaira, Japan). Wild-type ($Sgca^{+/+}$) and $Sgca^{-/-}$ mice (Burnham Institute, La Jolla, CA) were used. The TA muscles of 10-day-old (neonate) and 7-week-old (adult) $Sgca^{-/-}$ mice were transduced with 1×10^{11} vector genomes (VG) (10 μl) and 5×10^{11} VG (50 μl), respectively, of rAAV2- or rAAV8-α-SG, using 29-gauge needles.

Transgene expression analyses

Histological and immunohistochemical analyses were performed as described (Imamura *et al.*, 2000; Yuasa *et al.*, 2002). Cryosections (6 μm thick) were prepared from frozen muscle.

For colorimetric immunodetection of α-SG, blocked cryosections were incubated with a 1:1000 dilution of rabbit polyclonal anti-α-SG (Araishi *et al.*, 1999) for 1 hr at room temperature. The signal was visualized with a VECTASTAIN ABC kit (Vector Laboratories, Burlingame, CA) and then counterstained with hematoxylin and eosin (H&E). Stained sections were photographed with a light microscope (Leica, Heidelberg, Germany) using DP70 image scanning software (Olympus, Tokyo, Japan).

For fluorescence immunohistochemical detection of SGs, cryosections were fixed by immersion in cold acetone at –20°C for 5 min. After blocking with 2% casein in Tris-buffered saline (TBS, pH 7.4) at room temperature for 1 hr, α-SG was detected with rabbit polyclonal anti-α-SG (1:1000 dilution) (Araishi *et al.*, 1999). β-, γ-, and δ-SGs were detected with mouse monoclonal anti-β-SG (NCL-b-SARC, 1:50 dilution; Novocastra Laboratories, Newcastle-upon-Tyne, UK), anti-γ-SG (1:50 dilution), and anti-δ-SG (DSG-1; 1:50 dilution), respectively, after blocking with an M.O.M. kit (Vector Laboratories). Mouse monoclonal antibodies against γ-SG and δ-SG (DSG-1) were generated in our laboratory (Yamamoto *et al.*, 1994; Noguchi *et al.*, 1999). The signal was visualized with Alexa 488-conjugated anti-rabbit and anti-mouse IgG antibodies (Invitrogen Molecular Probes, Eugene, OR). Fluorescence signals were observed with a confocal laser-scanning microscope (Leica TCS SP; Leica).

Sodium dodecyl sulfate–polyacrylamide gel electrophoresis (SDS–PAGE) and protein transfer to a polyvinylidene di-

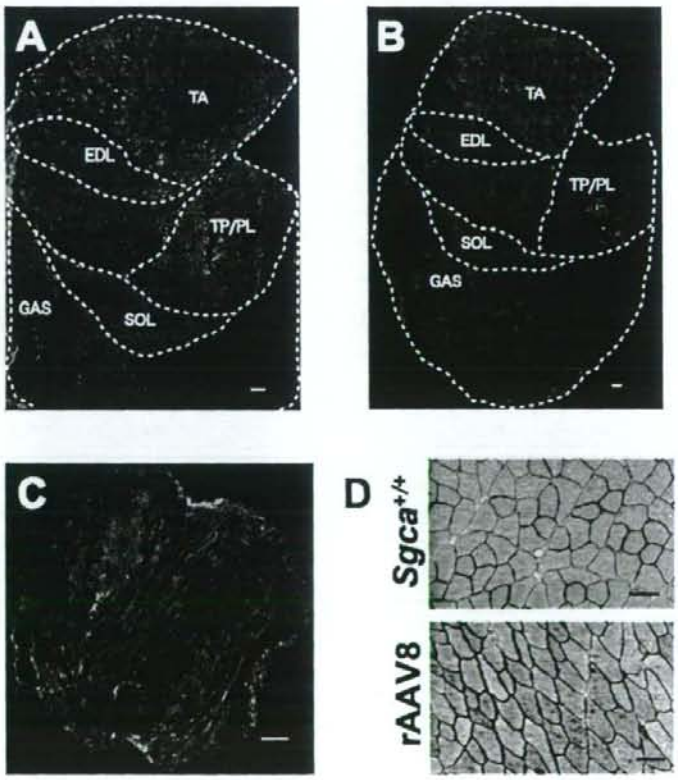

FIG. 2. Extensive α-SG expression after injection of rAAV8-α-SG into TA muscles of 7-week-old α-SG-deficient mice. Right TA muscles of adult $Sgca^{-/-}$ or $Sgca^{+/+}$ mice were transduced with 5×10^{11} VG of rAAV8-α-SG. Four weeks after rAAV8 injection, a cross-section of the right hind limb muscles (rAAV8-injected) (**A**), left contralateral hind limb muscles (**B**), and cardiac apex (**C**) were labeled by indirect immunofluorescence, using α-SG antibody (green). Scale bars: (**A** and **B**) 500 μm; (**C**) 100 μm. Note the widespread expression of α-SG in the hind limb muscles and cardiac muscle of rAAV8-α-SG-injected mice. (**D**) Cross-sections of TA muscle from $Sgca^{+/+}$ and rAAV8-injected $Sgca^{+/+}$ (rAAV8) mice were immunolabeled with α-SG antibody and counterstained with hematoxylin and eosin. Overexpression of α-SG caused no cytotoxic reactions in $Sgca^{+/+}$ muscle. Scale bars (**D**): 50 μm.

fluoride (PVDF) membrane were performed as described by Laemmli (1970) and Kyhse-Andersen (1984), respectively. Protein concentrations were determined with a protein assay kit (Bio-Rad, Hercules, CA) with bovine serum albumin as a standard.

Transgene copy number analyses

Cryosections of mouse hind limb muscle were collected for vector copy number analysis by quantitative PCR. After DNA extraction by successive treatments with RNase and proteinase K, viral genomes were quantified by a real-time PCR assay using SYBR *Premix Ex Taq* (TaKaRa Bio). The real-time PCR was carried out for 40 cycles, with each cycle consisting of 95°C for 5 sec, 60°C for 10 sec, 72°C for 10 sec, and 75°C for 10 sec. Oligonucleotide primers for this assay were 5'-CTCTAGAGGATCCGGTACTCGAGGAAC-3' (SD/SA sites) and 5'-AGAGGAGTCCAGAAGAGTGTCTCAGCC-3' (human α-SG gene) for the α-SG gene in the rAAV2 genome and 5'-TGCCATGAGCAGCCCATTTTG-3' and 5'-ATAACATCGCGGTGGCTCAGG-3' for the slug promoter. The slug promoter was used for normalization of data across samples.

Analysis of toxicity

Blood was obtained from a murine heart. Serum alanine aminotransferase, γ-glutamyl transpeptidase, albumin, and total protein concentration were determined with a Fuji Dri-Chem slide system (Fujifilm, Tokyo, Japan).

Muscle physiological function

TA and extensor digitorum longus (EDL) muscles were exposed by removal of overlying connective tissue (Xiao *et al.*, 2000; Yoshimura *et al.*, 2004; Imamura *et al.*, 2005). Both tendons of the TA and EDL muscles were cut from their insertions and secured with 5-0 silk sutures. Muscles were mounted in a vertical tissue chamber containing physiological salt solution (150 m*M* NaCl, 4 m*M* KCl, 1.8 m*M* $CaCl_2$, 1 m*M* $MgCl_2$, 5 m*M* HEPES, 5.6 m*M* glucose [pH 7.4], and 0.02 m*M* D-tubocurarine) maintained at 37°C with continuous aeration. The chamber was connected to a force transducer (UL-10GR; Minerva, Nagano, Japan) and a length servosystem (MM-3; Narishige, Tokyo, Japan). Electrical stimulation (SEN3301; Nihon Kohden, Tokyo, Japan) was delivered through a pair of platinum wires placed on both sides of the muscle. The muscle fiber length was adjusted incrementally with a micropositioner until peak isometric twitch force responses were obtained (i.e., optimal fiber length L_o). L_o was measured with a microcaliper. Maximal tetanic force (P_o) was induced by stimulation frequencies of 125 pulses per second, delivered in trains of 500-msec duration with 2-min intervals between each train. The muscle was weighed, rapidly frozen in liquid nitrogen-cooled isopentane, and stored at –80°C for further analysis. All forces were normalized to the physiological cross-section area (CSA), which was estimated on the basis of the following formula: muscle wet weight (in mg)/[L_o (in mm) × 1.06 (in mg/mm^3)]. The estimated CSA was used to determine specific tetanic (P_o/CSA) force of the muscle. Data are presented as means ± SE. Differences between groups were assessed by Student *t* test.

Exercise tolerance tests

Mice were subjected to an exhaustion treadmill test (Mourkioti *et al.*, 2006). Each mouse was placed on the belt of a four-lane motorized treadmill (MK-680; Muromachi Kikai, Tokyo, Japan) supplied with shocker plates. The treadmill was run at an inclination of 7 degrees at 5 m/min for 5 min, after which the speed was increased by 1 m/min every minute. The test was terminated when the mouse remained on the shocker plate for more than 20 sec without attempting to reengage the treadmill, and the time to exhaustion was determined.

Results

Expression of α-SG after injection of rAAV2- or rAAV8-α-SG into TA muscles of neonatal α-SG-deficient mice

We constructed rAAV2- and rAAV8-α-SG expressing human α-SG cDNA under the control of the ubiquitous CMV promoter, and injected 1×10^{11} VG into the right TA muscle of neonatal Sgca$^{-/-}$ mice (Fig. 1A). Neonatal Sgca$^{-/-}$ mice showed no obvious dystrophic changes, whereas adult (>4 weeks old) Sgca$^{-/-}$ skeletal muscles showed active cycles of the degeneration–regeneration process. In the hind limb muscles of 5-week-old Sgca$^{-/-}$ mice, α-SG-positive

TABLE 1. EFFECT OF rAAV2- AND rAAV8-α-SARCOGLYCAN ADMINISTRATION ON THE LIVER FUNCTION OF ADULT Sgca$^{-/-}$ MICE 4 WEEKS AFTER INJECTION[a,b]

	Number of mice	*ALT (U/liter)*	*γ-GTP (U/liter)*	*ALB (g/dl)*	*TP (g/dl)*
Sgca$^{+/+}$	3	26.67 ± 8.50[c]	<10	2.43 ± 0.21	4.80 ± 0.20
Sgca$^{-/-}$	3	145.33 ± 22.22	<10	2.33 ± 0.23	4.60 ± 0.42
rAAV2-injected Sgca$^{-/-}$	3	149 ± 9[d]	<10	2.10 ± 0.44	4.00 ± 0.53
rAAV8-injected Sgca$^{-/-}$	3	124 ± 15.10[e]	<10	2.03 ± 0.25	4.60 ± 0.89

Abbreviations: ALT/GPT, alanine aminotransferase/glutamic pyruvic transaminase; γ-GTP, γ-glutamyl transpeptidase; ALB, albumin; TP, total protein.

[a]Data represent means ± SE.

[b]The *p* values indicate statistical significance. Significant differences from the ALT/GPT level of Sgca$^{-/-}$ mice are indicated.

[c]$p < 0.001$.

[d]$p = 0.797$.

[e]$p = 0.229$.

fibers were not observed and the active cycle of muscle degeneration–regeneration was present (Fig. 1B). Four weeks after a single intramuscular injection of rAAV2-α-SG, α-SG was expressed only in a limited area of rAAV2-injected TA muscle (Fig. 1C and E). Analysis of TA muscle showed that less than 10% of muscle fibers were α-SG positive ($p < 0.01$; Fig. 1E).

In contrast, after rAAV8-α-SG injection, α-SG-positive fibers were widely spread in rAAV8-injected hind limb muscles, including the TA, extensor digitorum longus (EDL), soleus (SOL), gastrocnemius (GAS), and plantaris (PL)/tibialis posterior (TP) muscles (Fig. 1D). Analysis of the TA, EDL, and SOL muscles showed 62.3 ± 20.2, 79.5 ± 11.0, and 74.2 ± 11.2% α-SG-positive fibers, respectively ($p < 0.01$, $p < 0.001$, and $p < 0.001$; Fig. 1E). The expression of α-SG in rAAV8-α-SG-injected TA muscle and surrounding muscles persisted more than 7 months (data not shown).

Expression of α-SG after injection of rAAV2-α-SG or rAAV8-α-SG into TA muscles of adult α-SG-deficient mice

Adult Sgca$^{-/-}$ mice (>4 weeks old) showed active cycles of the degeneration–regeneration process and had a mature immune system. To investigate whether injection of rAAV2-α-SG or rAAV8-α-SG could induce stable expression of α-SG in adult Sgca$^{-/-}$ skeletal muscle without cytotoxicity and immune response, we injected 5×10^{11} VG of rAAV2-α-SG or rAAV8-α-SG into the right TA muscles of adult Sgca$^{-/-}$ mice. Four weeks after rAAV2-α-SG injection, we did not observe α-SG-positive fibers in the right TA muscle (data not shown). rAAV2-α-SG-injected TA muscles showed the degeneration–regeneration process. In contrast, after rAAV8-α-SG injection, we observed numerous α-SG-positive fibers in the entirety of rAAV8-injected hind limb muscles (Fig. 2A). Moreover, α-SG-positive fibers were detected even in contralateral hind limb muscles and cardiac muscle (Fig. 2B and C). In particular, when rAAV8-α-SG was injected into the TA muscle of Sgca$^{+/+}$ mice, we observed no pathological changes in the injected hind limb muscles 4 weeks after injection (Fig. 2D). No signs of tissue damage were found in regions where α-SG was detected after injection of rAAV8-α-SG. α-SG-positive myofibers retained normal morphology up to 4 weeks after injection. In addition, to examine whether rAAV2-α-SG and rAAV8-α-SG administration affect liver function, we measured the serum level of liver-related isozymes including alanine aminotransferase (ALT), γ-glu-

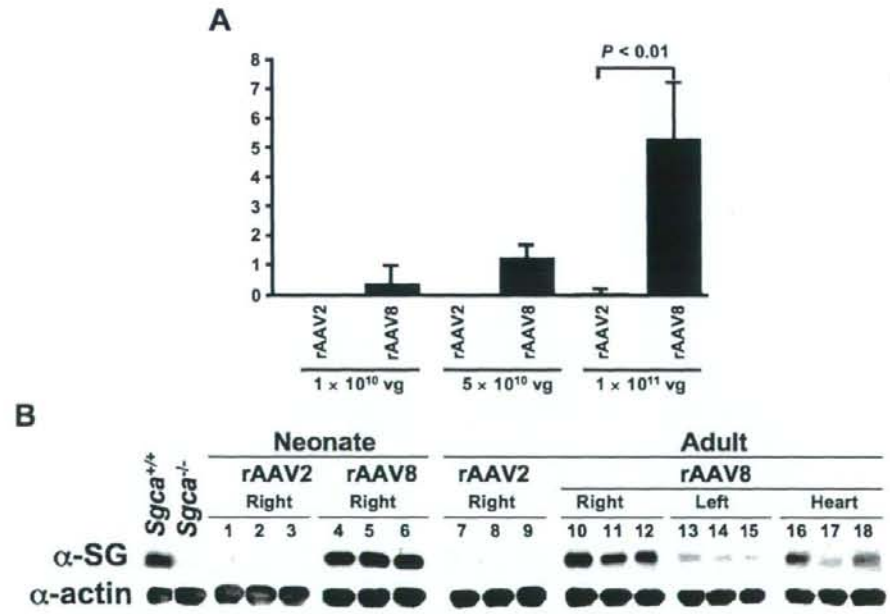

FIG. 3. Immunoblot analysis of α-SG in rAAV-injected α-SG-deficient muscles. Expression of α-SG in the hind limb muscles and heart of Sgca$^{-/-}$ mice was examined 4 weeks after rAAV injection, by real-time PCR and Western blot. (**A**) Real-time PCR was performed in duplicate to quantitate transgene copy number in each hind limb muscle after a single intramuscular administration of rAAV2-α-SG and rAAV8-α-SG. The right TA muscle of neonatal Sgca$^{-/-}$ mice was transduced with vector at 1×10^{10}, 5×10^{10}, and 1×10^{11} VG. Results are represented as vector copy number per diploid genome together with standard errors of mean. p Values are indicated and show a significant difference between rAAV2- and rAAV8-injected Sgca$^{-/-}$ mice ($p < 0.001$). (**B**) The right TA muscles of Sgca$^{-/-}$ mice were transduced with 1×10^{11} VG (neonates) or 5×10^{11} VG (adults) of rAAV2-α-SG (lanes 1–3 and 7–9) or rAAV8-α-SG (lanes 4–6 and 10–18). Ten-microgram samples of muscle lysates were separated by 10% SDS–PAGE. Faint bands were detected in the contralateral hind limb muscles of rAAV8-α-SG-injected mice. Adult Sgca$^{+/+}$ and Sgca$^{-/-}$ hind limb muscle lysates were used as positive and negative controls, respectively. The α-SG antibody detected a 50-kDa band. α-Sarcomeric actin is shown as a loading control.

tamyl transpeptidase (γ-GTP), albumin (ALB), and total protein (TP) in rAAV2-α-SG- and rAAV8-α-SG-injected Sgca$^{-/-}$ mice. Because skeletal muscle contains isozymes of creatine kinase, lactate dehydrogenase, aspartate aminotransferase, and ALT, these may be released into the blood stream after muscle necrosis (Janssen *et al.*, 1989); the ALT level in Sgca$^{-/-}$ mice was 5.4-fold higher than that in Sgca$^{+/+}$ mice ($p < 0.001$; Table 1). The ALT level in rAAV8-injected Sgca$^{-/-}$ mice was slightly lower than that in Sgca$^{-/-}$ mice. The levels of other liver-related proteins, including γ-GTP, ALB, and TP, were not significantly different between Sgca$^{-/-}$ and rAAV2-α-SG- and rAAV8-α-SG-injected Sgca$^{-/-}$ mice.

Tropism of rAAV2- and rAAV8-α-SG in α-SG-deficient mice

To investigate whether there is any difference in tissue tropism between rAAV2 and rAAV8, we determined the vector copies per diploid genome (C/DG) between the two vectors in injected skeletal muscle by a quantitative, real-time PCR assay. We injected neonatal Sgca$^{-/-}$ mice with either rAAV2-α-SG or rAAV8-α-SG at three different doses (1×10^{10}, 5×10^{10}, or 1×10^{11} VG/mouse) via the TA muscle ($n = 3$ per group). At a dose of 1×10^{11} VG/mouse, we detected rAAV2-α-SG and rAAV8-α-SG vector genomes in skeletal muscle at levels of 0.05 ± 0.03 and 5.33 ± 1.88 C/DG, respectively ($p < 0.01$; Fig. 3A). Increasing doses of rAAV8-α-SG resulted in increased levels of transgene expression. Higher transduction efficiency was observed with rAAV8-α-SG when large amounts of vector were used. Moreover, to evaluate the amount of α-SG in rAAV2-α-SG- or rAAV8-α-SG-injected skeletal muscles of Sgca$^{-/-}$ mice, we performed Western blot analysis. Four weeks after injection of rAAV2-α-SG into the TA muscle of neonatal and adult Sgca$^{-/-}$ mice, α-SG was almost undetectable (Fig. 3B). In contrast, when rAAV8-α-SG was injected into the right TA muscle of neonatal Sgca$^{-/-}$ mice, the amount of α-SG in rAAV8-transduced muscles was 3.5-fold higher than that in Sgca$^{+/+}$ muscles. When transduced in adulthood, the expression level of α-SG in the TA muscle of Sgca$^{-/-}$ mice was almost equal to that in Sgca$^{+/+}$ muscle. In addition, α-SG was detected in contralateral hind limb muscles and the heart after injection of rAAV8-α-SG into the TA muscle (Fig. 3B).

rAAV8-mediated α-SG expression ameliorated muscle pathology

A defect in any one of the four SGs can disrupt the entire SG complex in LGMD 2C-2F patients. Thus, we investigated the presence of a SG complex in the sarcolemma 4 weeks after injection of rAAV8-α-SG into the TA muscle of neonatal Sgca$^{-/-}$ mice. Immunostaining of rAAV8-α-SG-injected TA muscle with anti-SGs antibodies revealed that restoration of α-SG expression accompanied the sarcolemmal expression of other components of the SG complex, that is, β-, γ-, and δ-SG (Fig. 4). Moreover, 4 weeks after rAAV8-α-SG injection, H&E staining demonstrated considerable amelioration of the muscle pathology of rAAV8-injected TA muscles (Fig. 5A), and of surrounding EDL, SOL, GAS, and TP/PL muscles (data not shown). In contrast, uninjected and rAAV2-α-SG-injected muscles of Sgca$^{-/-}$ mice still showed signs of muscle degeneration and regeneration. To evaluate the amelioration of the dystrophic phenotype (Morgan *et al.*, 1990; Duclos *et al.*, 1998; Li *et al.*, 1999; Allamand *et al.*, 2000; Dressman *et al.*, 2002), we counted centrally nucleated myofibers in rAAV8-α-SG-injected muscles 4 months after injection (Fig. 5B). Sgca$^{-/-}$ hind limb muscles showed approximately 90% centrally nucleated myofibers. In contrast, rAAV8-α-SG-injected TA and ipsilateral EDL and SOL muscles showed

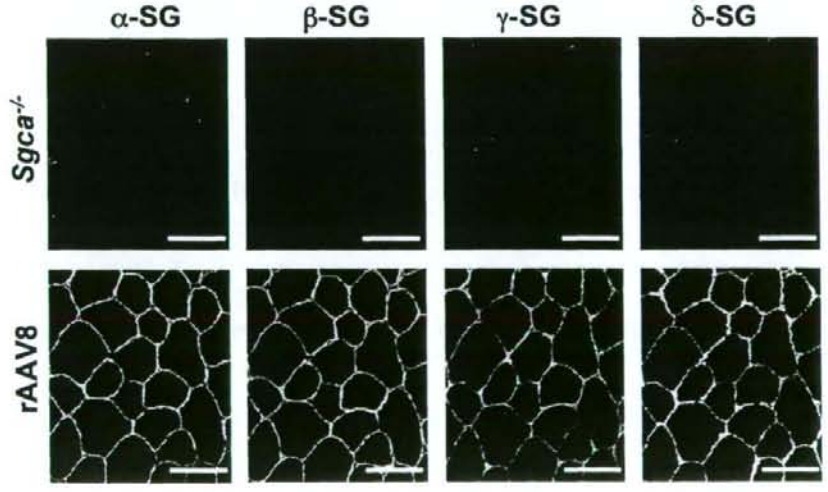

FIG. 4. Complete restoration of sarcoglycan expression at the sarcolemma of α-SG-deficient muscle after rAAV8-α-SG injection. Right TA muscles of neonatal Sgca$^{-/-}$ mice were injected with 1×10^{11} VG of rAAV8-α-SG. Untreated and rAAV8-injected Sgca$^{-/-}$ TA muscles (*top* and *bottom*, respectively) were labeled by indirect immunofluorescence, using specific antibodies against β-SG, γ-SG, or δ-SG. Untreated Sgca$^{-/-}$ muscle showed a secondary loss of SGs from the sarcolemma. Four weeks after injection, SGs were expressed in rAAV8-injected Sgca$^{-/-}$ muscle. Scale bars: 50 μm.

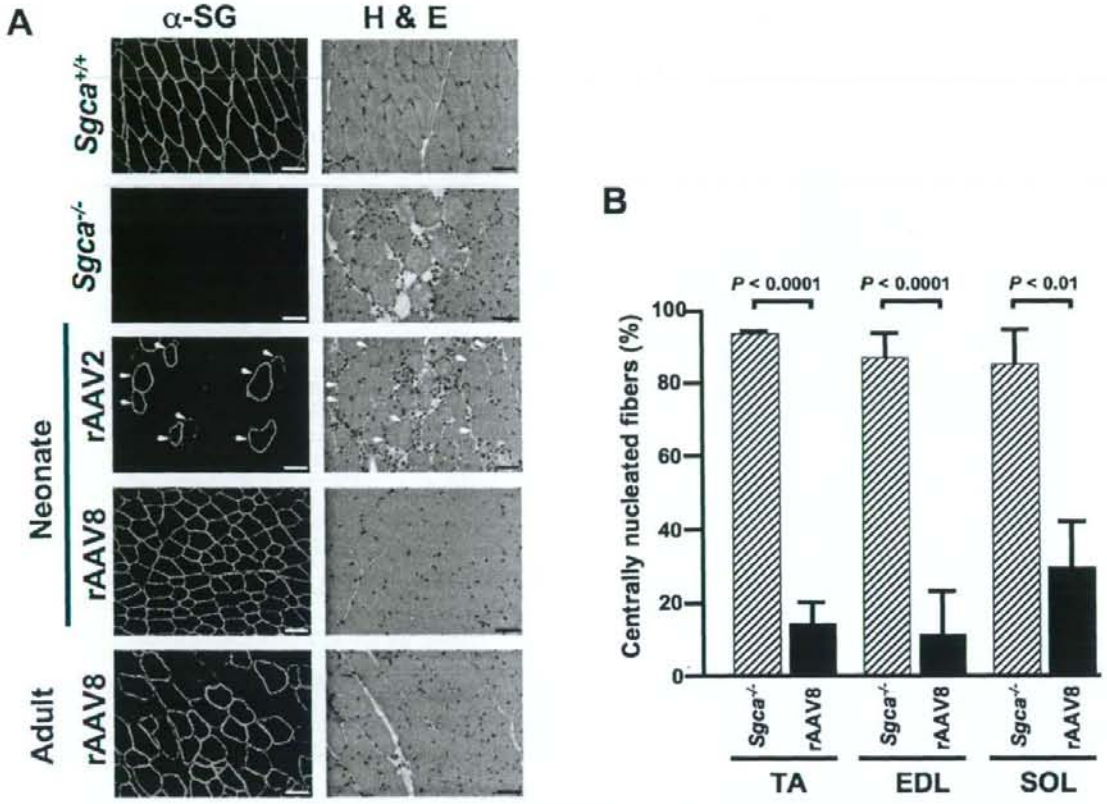

FIG. 5. Reduction of muscle degeneration in α-SG-deficient mice after rAAV8-α-SG-mediated gene transfer. (**A**) Right TA muscles of neonatal or adult Sgca$^{-/-}$ mice were transduced with 1×10^{11} VG (neonates) or 5×10^{11} VG (adults) of rAAV2-α-SG or rAAV8-α-SG. Four weeks after rAAV injection, serial cross-sections of Sgca$^{+/+}$, Sgca$^{-/-}$, and rAAV2- or rAAV8-injected Sgca$^{-/-}$ TA muscles (rAAV2 and rAAV8, respectively) were labeled by indirect immunofluorescence, using α-SG antibody (*left*, green), and stained with hematoxylin and eosin (H&E) (*right*). rAAV8-injected Sgca$^{-/-}$ TA muscles showed no signs of muscle degeneration. Arrowheads indicate α-SG-positive fibers. Scale bars: 50 μm. (**B**) Percentages of centrally nucleated myofibers in Sgca$^{-/-}$ skeletal muscles 4 months after injection of rAAV8-α-SG. Right TA muscles of neonatal Sgca$^{-/-}$ mice were transduced with 1×10^{11} VG of rAAV8-α-SG. Centrally nucleated myofibers among more than 200 total myofibers were counted in randomly selected H&E-stained cross-sections of the hind limb from Sgca$^{-/-}$ mice (hatched columns) and rAAV8-α-SG-injected Sgca$^{-/-}$ mice (solid columns) ($n = 3$ for each group). The percentage of centrally nucleated myofibers in rAAV8-α-SG-injected Sgca$^{-/-}$ mice was significantly lower than that in untreated Sgca$^{-/-}$ mice. p Values showed a statistically significant difference between Sgca$^{-/-}$ mice and rAAV8-injected Sgca$^{-/-}$ mice ($p < 0.0001$ for TA, $p < 0.0001$ for EDL, and $p < 0.01$ for SOL).

13.2 ± 7.3, 10.4 ± 10.4, and 29.1 ± 12.9% centrally nucleated myofibers, respectively ($p < 0.0001$, $p < 0.0001$, and $p < 0.0023$, respectively; Fig. 5B). The percentage of centrally nucleated myofibers in rAAV8-injected hind limb was significantly lower than that of Sgca$^{-/-}$ muscle, indicating that full recovery of the SG complex at the sarcolemma of Sgca$^{-/-}$ mice corrected the underlying biochemical deficiency and consequently restored the integrity of the muscle membrane.

rAAV-8-mediated α-SG expression improves contractile force and reverses muscle hypertrophy of α-SG-deficient muscle

A major functional deficit in muscular dystrophy patients is the loss of muscle strength. In our previous physiological study of muscular dystrophy model animals, we confirmed profound muscle force deficits in TA muscle (Yoshimura *et al.*, 2004; Imamura *et al.*, 2005).

A deficiency of α-SG decreases the contractile force of affected muscles (Danieli-Betto *et al.*, 2005; Imamura *et al.*, 2005). To evaluate whether rAAV8-α-SG transfer might improve Sgca$^{-/-}$ muscle physiological function, we measured the contractile force of rAAV8-injected Sgca$^{-/-}$ TA and EDL muscles. TA and EDL muscles were carefully separated from the hind limb and subjected to *in vitro* electrophysiological stimulation and contractile measurement on a force transducer. First, the right TA muscles of neonatal Sgca$^{-/-}$ mice were transduced with 1×10^{11} VG of rAAV8-α-SG. At the age of 5 months, the specific tetanic force of untreated Sgca$^{+/+}$ and Sgca$^{-/-}$ TA muscles was 17.3 ± 4.5 and 8.9 ±

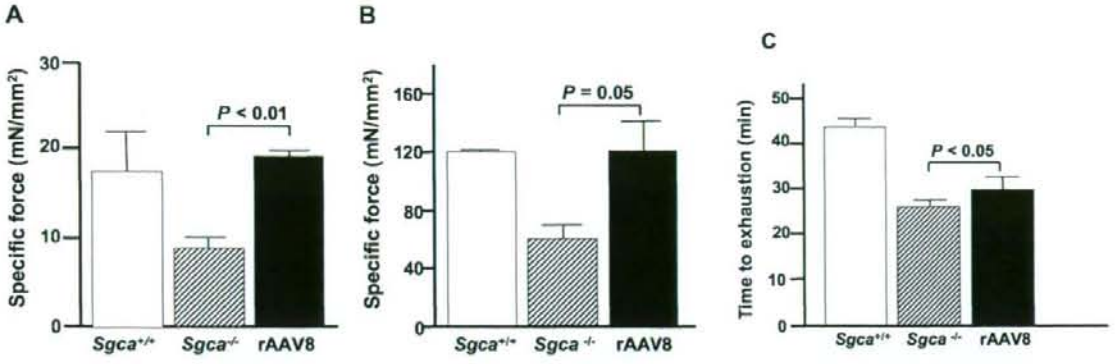

FIG. 6. Recovery of contractile force of α-SG-deficient muscle after transduction with rAAV8-α-SG. Right TA muscles of neonatal or adult Sgca$^{-/-}$ mice were transduced with 1×10^{11} VG (neonates) or 5×10^{11} VG (adults) of rAAV8-α-SG, and tetanic forces and time to exhaustion were assessed *in vitro* and *in vivo*. (**A**) Specific tetanic force of TA muscles from Sgca$^{+/+}$ (open column, $n = 3$), untreated Sgca$^{-/-}$ (hatched column, $n = 3$), and rAAV8-α-SG-injected Sgca$^{-/-}$ mice (solid column, $n = 3$). The right TA muscles of neonatal Sgca$^{-/-}$ mice were transduced with 1×10^{11} VG of rAAV8-α-SG, and the tetanic forces of TA muscles were assessed *in vitro* 5 months after injection. (**B**) Specific tetanic force of EDL muscles from Sgca$^{+/+}$ (open column, $n = 3$), untreated Sgca$^{-/-}$ (hatched column, $n = 3$), and rAAV8-α-SG-injected Sgca$^{-/-}$ mice (solid column, $n = 4$). The right TA muscles of adult Sgca$^{-/-}$ mice were transduced with 5×10^{11} VG of rAAV8-α-SG, and the tetanic forces of EDL muscles were assessed *in vitro* 10 weeks after injection. The p values show a statistically significant difference between Sgca$^{-/-}$ mice and rAAV8-injected Sgca$^{-/-}$ mice ($p < 0.01$ for TA, and $p = 0.05$ for EDL). (**C**) Time to exhaustion in treadmill test: Sgca$^{+/+}$ (open column, $n = 3$), untreated Sgca$^{-/-}$ (hatched column, $n = 4$), and rAAV8-α-SG-injected Sgca$^{-/-}$ mice (solid column, $n = 4$). The right TA muscles of adult Sgca$^{-/-}$ mice were transduced with 5×10^{11} VG of rAAV8-α-SG, and the tetanic forces of EDL muscles were assessed *in vitro* 10 weeks after injection. The p values show a statistically significant difference between Sgca$^{-/-}$ mice and rAAV8-injected Sgca$^{-/-}$ mice ($p < 0.05$).

1.2 mN/mm^2, respectively, whereas that of rAAV8-injected Sgca$^{-/-}$ TA muscle was 19.4 ± 0.7 mN/mm^2 ($p < 0.01$; Fig. 6A and Table 2). Furthermore, we assessed the improvement of EDL muscle after rAAV8-α-SG injection in adulthood. rAAV8-α-SG (5×10^{11} VG) was injected into the right TA muscle of adult Sgca$^{-/-}$ mice. We measured the contractile force of the EDL muscle surrounding rAAV8-injected TA muscle 10 weeks after injection. The specific tetanic forces of Sgca$^{+/+}$ and Sgca$^{-/-}$ EDL muscles were 121.5 ± 1.6 and 61.74 ± 8.33 mN/mm^2, and that of rAAV8-injected Sgca$^{-/-}$ EDL muscle was 121.15 ± 22.12 mN/mm^2 ($p = 0.05$; Fig. 6B and Table 2). Consequently, the specific tetanic force of animals injected with rAAV8-α-SG was 2-fold higher than that of uninjected Sgca$^{-/-}$ TA muscle ($p < 0.01$, and $p = 0.05$; Fig. 6A and B, Table 2).

In addition to the drastic improvement in contractile force of rAAV8-α-SG-injected TA muscle, the weight of rAAV8-α-SG-injected TA and EDL muscles as a percentage of body weight was comparable to those of Sgca$^{+/+}$ muscle and much smaller than those of their untreated counterparts (Table 2), suggesting that rAAV8-α-SG treatment reduced the muscle hypertrophy of Sgca$^{-/-}$ muscle. Moreover, we investigated whether α-SG expression in Sgca$^{-/-}$ muscle effectively increases the physical performance of the muscle. In an enforced treadmill test, the exhaustion times of Sgca$^{-/-}$ and rAAV8-α-SG injected Sgca$^{-/-}$ mice were 25.9 ± 2.0 and 30 ± 2.6 min ($p < 0.05$; Fig. 6C). rAAV8-injected Sgca$^{-/-}$ mice demonstrated increased exercise time before reaching exhaustion and could run longer distances.

Discussion

In this paper, we have presented evidence that a single intramuscular injection of a rAAV8 vector expressing human α-SG cDNA via a CMV promoter could achieve efficient therapeutic effects in a dystrophic animal model of LGMD 2D.

When rAAV8-α-SG was administered to neonatal Sgac$^{-/-}$ mice, we observed extensive α-SG transduction in the hind limb muscles, including the TA, EDL, SOL, and GAS muscles. In the case of rAAV8 injection of adult Sgac$^{-/-}$ mice, α-SG was expressed not only in all of the hind limb muscles and but also in cardiac muscle. A similar profile was further confirmed in a study by Wang and coworkers, in which they delivered more potent double-stranded rAAV8 vectors into adult and neonatal mice. The rAAV8 vector is more stable in the bloodstream than other rAAV serotypes when administered intravascularly and extravascularly (Wang *et al.*, 2005). The 37/67-kDa laminin receptor (LamR) has been identified as the host cell receptor for the AAV8 vector (Akache *et al.*, 2006). LamR is widely expressed in human tissues, where it is normally involved in interactions of extracellular laminin-1 with proteases and the cell (Ardini *et al.*, 1997, 2002). Furthermore, the rAAV8 vector might be able to cross the capillary endothelial cell barrier and transduce remote organs with high efficiency (Inagaki *et al.*, 2006). However, the detailed mechanism of rAAV8-mediated cell recognition and transduction has yet to be fully elucidated.

In the present study, we demonstrated that rAAV8-α-SG transduced skeletal muscle about 100-fold more compared with rAAV2-α-SG. In addition, rAAV8-α-SG-injected

TABLE 2. CONTRACTILE PROPERTIES OF rAAV8-INJECTED α-SARCOGLYCAN DEFICIENT MUSCLE[a,b]

	Injection age	*Number of mice*	*Tissue*	*Muscle length* (L_o, *mm*)	*Muscle weight* (*mg*)	*Tissue weight* (*% of body weight*)	*CSA* (mm^2)	*Maximal contraction* (P_o, *mN*)	*Specific force* (mN/mm^2)
$Sgca^{+/+}$	10-day-old	3	TA	11	56.1 ± 2.9	0.185 ± 0.004	4.81 ± 0.14	82.3 ± 19.2	17.3 ± 4.5
$Sgca^{-/-}$	10-day-old	3	TA	11.5	68.1 ± 6.9	0.233 ± 0.023	5.61 ± 0.32	48.5 ± 4.0	8.9 ± 1.2
rAAV8-injected $Sgca^{-/-}$	10-day-old	3	TA	11.5	65.7 ± 8.2	0.224 ± 0.027	5.05 ± 0.46	103.8 ± 10.3	19.4 ± 0.7[c]
$Sgca^{+/+}$	7-week-old	3	EDL	14.83 ± 0.83	11.30 ± 0.46	0.044 ± 0.001	0.73 ± 0.07	88.3 ± 8.5	121.5 ± 1.6
$Sgca^{-/-}$	7-week-old	3	EDL	14	13.5 ± 0.48	0.047 ± 0.002	0.91 ± 0.03	56.94 ± 9.25	61.74 ± 8.33
rAAV8-Injected $Sgca^{-/-}$	7-week-old	4	EDL	14	10.7 ± 0.84	0.038 ± 0.003	0.72 ± 0.06[d]	84.04 ± 8.74	121.15 ± 22.12[e]

Abbreviations: CSA, tissue cross-sectional area; EDL, extensor digitorum longus; TA, tibialis anterior.
[a]Data represent means ± SE. Tissue weights were normalized to respective body weights.
[b]The *p* values indicate statistical significance between $Sgca^{-/-}$ mice and rAAV8-injected $Sgca^{-/-}$ mice.
[c]$p < 0.01$ when rAAV8 was injected into neonatal $Sgca^{-/-}$ TA muscle.
[d]$p \leq 0.05$ when rAAV8 was injected into adult $Sgca^{-/-}$ EDL muscle.
[e]$p \leq 0.05$ when rAAV8 was injected into adult $Sgca^{-/-}$ EDL muscle.

Sgca$^{-/-}$ mice did not demonstrate cytotoxic and immunological reactions for more than 7 months after injection. Transduction of α-SG in an LGMD 2D animal model by means of adenovirus, rAAV1, or rAAV2 vector was previously reported (Duclos *et al.*, 1998; Allamand *et al.*, 2000; Dressman *et al.*, 2002; Fougerousse *et al.*, 2007; Pacak *et al.*, 2007). In the two studies using the adenovirus vector, it was necessary to use neonatal animals to take advantage of the immaturity of the immune system and thereby to circumvent the strong immune response elicited by the adenoviral vector (Duclos *et al.*, 1998; Allamand *et al.*, 2000). The AAV vector, which has been more widely used, is nonpathogenic, has low immunogenicity, and has been shown to confer long-term gene expression in muscles of various species. Use of the ubiquitous CMV promoter would allow expression of the transgene in various cells. Therefore, expression of α-SG via rAAV1 and rAAV2, using the CMV promoter, induced an immune response, whereas those vectors introduced balanced expression of SGs within the injected Sgca$^{-/-}$ myofibers (Duclos *et al.*, 1998; Allamand *et al.*, 2000; Dressman *et al.*, 2002; Fougerousse *et al.*, 2007; Pacak *et al.*, 2007). Between 28 and 41 days after rAAV2 injection, a drastic decrease in α-SG expression occurred in the injected Sgca$^{-/-}$ muscle. In particular, numerous antigen-presenting cells in the dystrophic muscles could direct a strong immune response against the transgene product when the CMV promoter was used (Yuasa *et al.*, 2002). On the other hand, the AAV8 vector transduced antigen-presenting cells (such as dendritic cells) less efficiently than did the rAAV2 vector (Xin *et al.*, 2006). Consequently, gene transduction via the AAV2 vector with the CMV promoter might be less efficient than with rAAV8 and other AAV serotypes.

Because the CMV promoter elicits an immune response against the transgene product (Cordier *et al.*, 2001; Yuasa *et al.*, 2002; Liu *et al.*, 2004), several studies of rAAV-mediated transduction of striated musculature used the muscle creatine kinase (MCK), CK6, or SP6 promoter as a muscle-specific promoter (Gregorevic *et al.*, 2004; Yoshimura *et al.*, 2004; Zhu *et al.*, 2005). Transduction driven by a muscle-specific promoter was achieved without acute toxicological response. Moreover, to enable strong expression in striated muscle, another group created a hybrid promoter containing the MCK enhancer and the simian virus 40 promoter (MCK/SV40 promoter) (Takeshita *et al.*, 2007). The MCK/SV40 promoter yielded long-term (>6 months) expression of a human secretory alkaline phosphatase (huSEAP) reporter gene after electrotransfer of the plasmid into mice. In addition, selection of the rAAV serotype is important. rAAV9 has also been shown to be efficient in cardiac or skeletal muscle transduction (Inagaki *et al.*, 2006; Sarkar *et al.*, 2006).

Our study demonstrated improvement of the contractile force and decreased sensitivity to stretch and exhaustion time for exercise in Sgca$^{-/-}$ muscle after rAAV8-α-SG injection. Recovery of absolute maximal force and specific tetanic force is one of the barometers of amelioration. A dose of about 1×10^{11} VG (for neonates) or 5×10^{11} VG (for adults) in Sgca$^{-/-}$ TA muscle led to transduction of approximately >70% of hind limb muscles and was sufficient to increase the global force of the animal. We compared tetanic contractions of rAAV8-α-SG-injected muscles with those of Sgca$^{+/+}$ and Sgca$^{-/-}$ muscles. The contractile forces of rAAV8-injected Sgca$^{-/-}$ TA and EDL muscles were increased 2-fold compared with that of Sgca$^{-/-}$ muscles. Furthermore, the exercise treadmill test results for rAAV8-injected Sgca$^{-/-}$ mice were higher than those of Sgca$^{-/-}$ mice. This suggested that increased synthesis of α-SG had no adverse effects on SG complex formation, and that overexpression of α-SG might induce stability of the transmembrane without causing muscle pathology. In a therapeutic study using rAAV1 (Fougerousse *et al.*, 2007), injection of rAAV1 encoding α-SG cDNA via the C5-12 promoter (a muscle-specific promoter) into the artery of Sgca$^{-/-}$ mice increased the contractile force of EDL muscles 1.5-fold compared with that of Sgca$^{-/-}$ EDL muscles. Therefore, rAAV8 would be an effective tool for the delivery of therapeutic genes to skeletal muscles in the treatment of limb-girdle muscular dystrophy.

Acknowledgments

The authors greatly appreciate the technical support and helpful discussion provided by Ms. Kazue Kinoshita and Dr. Katsutoshi Yuasa. We thank Dr. Eva Engvall for providing the Sgca$^{-/-}$ mice. This work was supported by a Grant for Research on Nervous and Mental Disorders (16B-2) and by Health Science Research Grants for Research on the Human Genome and Gene Therapy (H16-genome-003) and for Research on Brain Science (H15-kokoro-021 and H18-kokoro-019) from the Ministry of Health, Labor, and Welfare; and by Grants in Aid for Scientific Research (16390418, 16590333, 18590392, and 19390383) from the Ministry of Education, Culture, Sports, Science, and Technology.

References

Akache, B., Grimm, D., Pandey, K., Yant, S.R., Xu, H., and Kay, M.A. (2006). The 37/67-kilodalton laminin receptor is a receptor for adeno-associated virus serotypes 8, 2, 3, and 9. J. Virol. 80, 9831–9836.

Allamand, V., Donahue, K.M., Straub, V., Davisson, R.L., Davidson, B.L., and Campbell, K.P. (2000). Early adenovirus-mediated gene transfer effectively prevents muscular dystrophy in α-sarcoglycan-deficient mice. Gene Ther. 7, 1385–1391.

Araishi, K., Sasaoka, T., Imamura, M., Noguchi, S., Hama, H., Wakabayashi, E., Yoshida, M., Hori, T., and Ozawa, E. (1999). Loss of the sarcoglycan complex and sarcospan leads to muscular dystrophy in β-sarcoglycan-deficient mice. Hum. Mol. Genet. 8, 1589–1598.

Ardini, E., Tagliabue, E., Magnifico, A., Buto, S., Castronovo, V., Colnaghi, M.I., and Menard, S. (1997). Co-regulation and physical association of the 67-kDa monomeric laminin receptor and the $\alpha_6\beta_4$ integrin. J. Biol. Chem. 272, 2342–2345.

Ardini, E., Sporchia, B., Pollegioni, L., Modugno, M., Ghirelli, C., Castiglioni, F., Tagliabue, E., and Menard, S. (2002). Identification of a novel function for 67-kDa laminin receptor: Increase in laminin degradation rate and release of motility fragments. Cancer Res. 62, 1321–1325.

Bonnemann, C.G., Modi, R., Noguchi, S., Mizuno, Y., Yoshida, M., Gussoni, E., McNally, E.M., Duggan, D.J., Angelini, C., and Hoffman, E.P. (1995). β-Sarcoglycan (A3b) mutations cause autosomal recessive muscular dystrophy with loss of the sarcoglycan complex. Nat. Genet. 11, 266–273.

Burton, M., Nakai, H., Colosi, P., Cunningham, J., Mitchell, R., and Couto, L. (1999). Coexpression of factor VIII heavy and light chain adeno-associated viral vectors produces biologically active protein. Proc. Natl. Acad. Sci. U.S.A. 96, 12725–12730.

Cordier, L., Gao, G.P., Hack, A.A., McNally, E.M., Wilson, J.M., Chirmule, N., and Sweeney, H.L. (2001). Muscle-specific promoters may be necessary for adeno-associated virus-mediated gene transfer in the treatment of muscular dystrophies. Hum. Gene Ther. 12, 205–215.

Danieli-Betto, D., Esposito, A., Germinario, E., Sandona, D., Martinello, T., Jakubiec-Puka, A., Biral, D., and Betto, R. (2005). Deficiency of α-sarcoglycan differently affects fast- and slow-twitch skeletal muscles. Am. J. Physiol. Regul. Integr. Comp. Physiol. 289, R1328–R1337.

Dressman, D., Araishi, K., Imamura, M., Sasaoka, T., Liu, L.A., Engvall, E., and Hoffman, E.P. (2002). Delivery of α- and β-sarcoglycan by recombinant adeno-associated virus: Efficient rescue of muscle, but differential toxicity. Hum. Gene Ther. 13, 1631–1646.

Duclos, F., Straub, V., Moore, S.A., Venzke, D.P., Hrstka, R.F., Crosbie, R.H., Durbeej, M., Lebakken, C.S., Ettinger, A.J., Van Der Meulen, J., Holt, K.H., Lim, L.E., Sanes, J.R., Davidson, B.L., Faulkner, J.A., Williamson, R., and Campbell, K.P. (1998). Progressive muscular dystrophy in α-sarcoglycan-deficient mice. J. Cell Biol. 142, 1461–1471.

Ervasti, J.M., Ohlendieck, K., Kahl, S.D., Gaver, M.G., and Campbell, K.P. (1990). Deficiency of a glycoprotein component of the dystrophin complex in dystrophic muscle. Nature 345, 315–319.

Eymard, B., Romero, N.B., Leturcq, F., Piccolo, F., Carrie, A., Jeanpierre, M., Collin, H., Deburgrave, N., Azibi, K., Chaouch, M., Merlini, L., Themar-Noel, C., Penisson, I., Mayer, M., Tanguy, O., Campbell, K.P., Kaplan, J.C., Tome, F.M., and Fardeau, M. (1997). Primary adhalinopathy (α-sarcoglycanopathy): Clinical, pathologic, and genetic correlation in 20 patients with autosomal recessive muscular dystrophy. Neurology 48, 1227–1234.

Fanin, M., Duggan, D.J., Mostacciuolo, M.L., Martinello, F., Freda, M.P., Soraru, G., Trevisan, C.P., Hoffman, E.P., and Angelini, C. (1997). Genetic epidemiology of muscular dystrophies resulting from sarcoglycan gene mutations. J. Med. Genet. 34, 973–977.

Fisher, K.J., Jooss, K., Alston, J., Yang, Y., Haecker, S.E., High, K., Pathak, R., Raper, S.E., and Wilson, J.M. (1997). Recombinant adeno-associated virus for muscle directed gene therapy. Nat. Med. 3, 306–312.

Fougerousse, F., Bartoli, M., Poupiot, J., Arandel, L., Durand, M., Guerchet, N., Gicquel, E., Danos, O., and Richard, I. (2007). Phenotypic correction of α-sarcoglycan deficiency by intra-arterial injection of a muscle-specific serotype 1 rAAV vector. Mol. Ther. 15, 53–61.

Gao, G., Vandenberghe, L.H., Alvira, M.R., Lu, Y., Calcedo, R., Zhou, X., and Wilson, J.M. (2004). Clades of adeno-associated viruses are widely disseminated in human tissues. J. Virol. 78, 6381–6388.

Gao, G.P., Alvira, M.R., Wang, L., Calcedo, R., Johnston, J., and Wilson, J.M. (2002). Novel adeno-associated viruses from rhesus monkeys as vectors for human gene therapy. Proc. Natl. Acad. Sci. U.S.A. 99, 11854–11859.

Greelish, J.P., SU, L.T., Lankford, E.B., Burkman, J.M., Chen, H., Konig, S.K., Mercier, I.M., Desjardins, P.R., Mitchell, M.A., Zheng, X.G., Leferovich, J., Gao, G.P., Balice-Gordon, R.J., Wilson, J.M., and Stedman, H.H. (1999). Stable restoration of the sarcoglycan complex in dystrophic muscle perfused with histamine and a recombinant adeno-associated viral vector. Nat. Med. 5, 439–443.

Gregorevic, P., Blankinship, M.J., Allen, J.M., Crawford, R.W., Meuse, L., Miller, D.G., Russell, D.W., and Chamberlain, J.S. (2004). Systemic delivery of genes to striated muscles using adeno-associated viral vectors. Nat. Med. 10, 828–834.

Imamura, M., Araishi, K., Noguchi, S., and Ozawa, E. (2000). A sarcoglycan–dystroglycan complex anchors Dp116 and utrophin in the peripheral nervous system. Hum. Mol. Genet. 9, 3091–3100.

Imamura, M., Mochizuki, Y., Engvall, E., and Takeda, S. (2005). ε-Sarcoglycan compensates for lack of α-sarcoglycan in a mouse model of limb-girdle muscular dystrophy. Hum. Mol. Genet. 14, 775–783.

Inagaki, K., Fuess, S., Storm, T.A., Gibson, G.A., McTiernan, C.F., Kay, M.A., Nakai, H., Sarkar, R., Mucci, M., Addya, S., Tetreault, R., Bellinger, D.A., Nichols, T.C., and Kazazian, H.H., Jr. (2006). Robust systemic transduction with AAV9 vectors in mice: Efficient global cardiac gene transfer superior to that of AAV8. Mol. Ther. 14, 45–53.

Iwata, Y., Nakamura, H., Mizuno, Y., Yoshida, M., Ozawa, E., and Shigekawa, M. (1993). Defective association of dystrophin with sarcolemmal glycoproteins in the cardiomyopathic hamster heart. FEBS Lett. 329, 227–231.

Janssen, G.M., Kuipers, H., Willems, G.M., Does, R.J., Janssen, M.P., and Geurten, P. (1989). Plasma activity of muscle enzymes: Quantification of skeletal muscle damage and relationship with metabolic variables. Int. J. Sports Med. 10(Suppl. 3), S160–S168.

Kessler, P.D., Podsakoff, G.M., Chen, X., McQuiston, S.A., Colosi, P.C., Matelis, L.A., Kurtzman, G.J., and Byrne, B.J. (1996). Gene delivery to skeletal muscle results in sustained expression and systemic delivery of a therapeutic protein. Proc. Natl. Acad. Sci. U.S.A. 93, 14082–14087.

Kyhse-Andersen, J. (1984). Electroblotting of multiple gels: A simple apparatus without buffer tank for rapid transfer of proteins from polyacrylamide to nitrocellulose. J. Biochem. Biophys. Methods 10, 203–209.

Laemmli, U.K. (1970). Cleavage of structural proteins during the assembly of the head of bacteriophage T4. Nature 227, 680–685.

Li, J., Dressman, D., Tsao, Y.P., Sakamoto, A., Hoffman, E.P., and Xiao, X. (1999). rAAV vector-mediated sarcoglycan gene transfer in a hamster model for limb girdle muscular dystrophy. Gene Ther. 6, 74–82.

Liu, Y.L., Mingozzi, F., Rodriguez-Colon, S.M., Joseph, S., Dobrzynski, E., Suzuki, T., High, K.A., and Herzog, R.W. (2004). Therapeutic levels of factor IX expression using a muscle-specific promoter and adeno-associated virus serotype 1 vector. Hum. Gene Ther. 15, 783–792.

McNally, E.M., Yoshida, M., Mizuno, Y., Ozawa, E., and Kunkel, L.M. (1994). Human adhalin is alternatively spliced and the gene is located on chromosome 17q21. Proc. Natl. Acad. Sci. U.S.A. 91, 9690–9694.

Morgan, J.E., Hoffman, E.P., and Partridge, T.A. (1990). Normal myogenic cells from newborn mice restore normal histology to degenerating muscles of the *mdx* mouse. J. Cell Biol. 111, 2437–2449.

Mourkioti, F., Kratsios, P., Luedde, T., Song, Y.H., Delafontaine, P., Adami, R., Parente, V., Bottinelli, R., Pasparakis, M., and Rosenthal, N. (2006). Targeted ablation of IKK2 improves skeletal muscle strength, maintains mass, and promotes regeneration. J. Clin. Invest. 116, 2945–2954.

Nigro, V., De Sa Moreira, E., Piluso, G., Vainzof, M., Belsito, A., Politano, L., Puca, A.A., Passos-Bueno, M.R., and Zatz, M. (1996). Autosomal recessive limb-girdle muscular dystrophy, LGMD2F, is caused by a mutation in the δ-sarcoglycan gene. Nat. Genet. 14, 195–198.

Noguchi, S., McNally, E.M., Ben Othmane, K., Hagiwara, Y., Mizuno, Y., Yoshida, M., Yamamoto, H., Bonnemann, C.G., Gussoni, E., Denton, P.H., Kyriakides, T., Middleton, L., Hen-

tati, F., Ben Hamida, M., Nonaka, I., Vance, J.M., Kunkel, L.M., and Ozawa, E. (1995). Mutations in the dystrophin-associated protein γ-sarcoglycan in chromosome 13 muscular dystrophy. Science 270, 819–822.

Noguchi, S., Wakabayashi, E., Imamura, M., Yoshida, M., and Ozawa, E. (1999). Developmental expression of sarcoglycan gene products in cultured myocytes. Biochem. Biophys. Res. Commun. 262, 88–93.

Pacak, C.A., Walter, G.A., Gaidosh, G., Bryant, N., Lewis, M.A., Germain, S., Mah, C.S., Campbell, K.P., and Byrne, B.J. (2007). Long-term skeletal muscle protection after gene transfer in a mouse model of LGMD-2D. Mol. Ther. 15, 1775–1781.

Sarkar, R., Mucci, M., Addya, S., Tetreault, R., Bellinger, D.A., Nichols, T.C., and Kazazian, H.H., Jr. (2006). Long-term efficacy of adeno-associated virus serotypes 8 and 9 in hemophilia a dogs and mice. Hum. Gene Ther. 17, 427–439.

Takeshita, F., Takase, K., Tozuka, M., Saha, S., Okuda, K., Ishii, N., and Sasaki, S. (2007). Muscle creatine kinase/SV40 hybrid promoter for muscle-targeted long-term transgene expression. Int. J. Mol. Med. 19, 309–315.

Wang, Z., Zhu, T., Qiao, C., Zhou, L., Wang, B., Zhang, J., Chen, C., Li, J., and Xiao, X. (2005). Adeno-associated virus serotype 8 efficiently delivers genes to muscle and heart. Nat. Biotechnol. 23, 321–328.

Wigler, M., Perucho, M., Kurtz, D., Dana, S., Pellicer, A., Axel, R., and Silverstein, S. (1980). Transformation of mammalian cells with an amplifiable dominant-acting gene. Proc. Natl. Acad. Sci. U.S.A. 77, 3567–3570.

Xiao, X., Li, J., and Samulski, R.J. (1996). Efficient long-term gene transfer into muscle tissue of immunocompetent mice by adeno-associated virus vector. J. Virol. 70, 8098–8108.

Xiao, X., Li, J., and Samulski, R.J. (1998). Production of high-titer recombinant adeno-associated virus vectors in the absence of helper adenovirus. J. Virol. 72, 2224–2232.

Xiao, X., Li, J., Tsao, Y.P., Dressman, D., Hoffman, E.P., and Watchko, J.F. (2000). Full functional rescue of a complete muscle (TA) in dystrophic hamsters by adeno-associated virus vector-directed gene therapy. J. Virol. 74, 1436–1442.

Xin, K.Q., Mizukami, H., Urabe, M., Toda, Y., Shinoda, K., Yoshida, A., Oomura, K., Kojima, Y., Ichino, M., Klinman, D., Ozawa, K., and Okuda, K. (2006). Induction of robust immune responses against human immunodeficiency virus is supported by the inherent tropism of adeno-associated virus type 5 for dendritic cells. J. Virol. 80, 11899–11910.

Yamamoto, H., Mizuno, Y., Hayashi, K., Nonaka, I., Yoshida, M., and Ozawa, E. (1994). Expression of dystrophin-associated protein 35DAG (A4) and 50DAG (A2) is confined to striated muscles. J. Biochem. 115, 162–167.

Yoshida, M., and Ozawa, E. (1990). Glycoprotein complex anchoring dystrophin to sarcolemma. J. Biochem. 108, 748–752.

Yoshimura, M., Sakamoto, M., Ikemoto, M., Mochizuki, Y., Yuasa, K., Miyagoe-Suzuki, Y., and Takeda, S. (2004). AAV vector-mediated microdystrophin expression in a relatively small percentage of *mdx* myofibers improved the *mdx* phenotype. Mol. Ther. 10, 821–828.

Yuasa, K., Sakamoto, M., Miyagoe-Suzuki, Y., Tanouchi, A., Yamamoto, H., Li, J., Chamberlain, J.S., Xiao, X., and Takeda, S. (2002). Adeno-associated virus vector-mediated gene transfer into dystrophin-deficient skeletal muscles evokes enhanced immune response against the transgene product. Gene Ther. 9, 1576–1588.

Zhu, T., Zhou, L., Mori, S., Wang, Z., McTiernan, C.F., Qiao, C., Chen, C., Wang, D.W., Li, J., and Xiao, X. (2005). Sustained whole-body functional rescue in congestive heart failure and muscular dystrophy hamsters by systemic gene transfer. Circulation 112, 2650–2659.

Address reprint requests to:
Dr. Shin'ichi Takeda or Dr. Takashi Okada
Department of Molecular Therapy
National Institute of Neuroscience, NCNP
4-1-1 Ogawa-higashi, Kodaira
Tokyo 187-8502, Japan

E-mail: takeda@ncnp.go.jp or t-okada@ncnp.go.jp

Received for publication January 4, 2008; accepted after revision May 14, 2008.

Published online: June 17, 2008.

Gene Therapy (2008), 1–5

www.nature.com/gt

SHORT COMMUNICATION

Atelocollagen-mediated local and systemic applications of myostatin-targeting siRNA increase skeletal muscle mass

N Kinouchi[1], Y Ohsawa[2], N Ishimaru[3], H Ohuchi[4], Y Sunada[2], Y Hayashi[3], Y Tanimoto[1], K Moriyama[1,5] and S Noji[4]

[1]*Department of Orthodontics and Dentofacial Orthopedics, Graduate School of Dentistry, The University of Tokushima, Tokushima, Japan;* [2]*Department of Internal Medicine, Division of Neurology, Kawasaki Medical School, Okayama, Japan;* [3]*Department of Oral Molecular Pathology, Institute of Health Bioscience, The University of Tokushima Graduate School, Tokushima, Japan and* [4]*Department of Life Systems, Institute of Technology and Science, The University of Tokushima, Tokushima, Japan*

RNA interference (RNAi) offers a novel therapeutic strategy based on the highly specific and efficient silencing of a target gene. Since it relies on small interfering RNAs (siRNAs), a major issue is the delivery of therapeutically active siRNAs into the target tissue/target cells in vivo. *For safety reasons, strategies based on vector delivery may be of only limited clinical use. The more desirable approach is to directly apply active siRNAs* in vivo. *Here, we report the effectiveness of* in vivo *siRNA delivery into skeletal muscles of normal or diseased mice through nanoparticle formation of chemically unmodified siRNAs with atelocollagen (ATCOL). ATCOL-mediated local application of siRNA targeting myostatin, a negative regulator of skeletal muscle growth, in mouse skeletal muscles or intravenously, caused a marked increase in the muscle mass within a few weeks after application. These results imply that ATCOL-mediated application of siRNAs is a powerful tool for future therapeutic use for diseases including muscular atrophy.*
Gene Therapy advance online publication, 6 March 2008; doi:10.1038/gt.2008.24

Keywords: *myostatin; RNA interference; atelocollagen; muscle; mouse; muscular dystrophy*

RNA interference (RNAi) is the process of sequence-specific, posttranscriptional gene silencing in plants and animals from flatworms to human,[1] which is mediated by ~22-nucleotide small interfering RNAs (siRNAs) generated from longer double-stranded RNA. Since it was demonstrated that siRNAs can intervene gene silencing in mammalian cells without induction of interferon synthesis or nonspecific gene suppression,[2] an increasing number of remedies utilizing highly specific siRNAs targeted against disease-causing or disease-promoting genes have been developed.[3] Effective delivery of active siRNAs to target organs or tissues is therefore the key to the development of RNAi as a broad therapeutic platform. For this purpose, different strategies have been used to deliver and achieve RNAi-mediated gene silencing *in vivo*;[3] for example, polymers represent a class of materials that meet the needs of a particular siRNA delivery system, condensing siRNAs into nano-sized particles taken up by cells.[4] However, some of the synthetic polymers, which have been used for delivery of nucleic acids, may trigger cell death in a variety of cell lines and thus suffer from limitations for its application in siRNA delivery *in vivo*.[4] On the other hand, atelocollagen (ATCOL), a pepsin-treated type I collagen lacking in telopeptides in N and C terminals that confer its antigenicity, has been shown to elicit an efficient delivery of chemically unmodified siRNAs to metastatic tumors *in vivo*.[5–7] In this study, we sought to examine the effectiveness of siRNA-ATCOL therapy for a nontumorous systemic disease, targeted against myostatin (growth/differentiation factor 8, GDF8), a negative regulator of skeletal muscle growth.[8]

Skeletal muscles are the crucial morphofunctional organs, and their atrophy causes severe conditions for life such as muscular dystrophies. Duchenne muscular dystrophy (DMD), for instance, is a severe muscle wasting disorder affecting 1 out of 3500 male birth.[9] There is currently no effective treatment, but gene therapy approaches are offering viable avenues for treatment development.[10] As one of therapeutic approaches, inhibition of myostatin by using anti-myostatin-blocking antibodies has been employed to increase muscle mass.[11] However, generating antibodies against recombinant target proteins is time consuming and requires a lot of efforts. Recently, we demonstrated that inhibition of myostatin by overexpression of the myostatin prodomain[12] prevented muscular atrophy and

Correspondence: Professor S Noji or Dr H Ohuchi, Department of Life Systems, Institute of Technology and Science, The University of Tokushima, 2-1 Minami-Jyosanjima-cho, Tokushima 770-8506, Japan.
E-mails: noji@bio.tokushima-u.ac.jp or hohuchi@bio.tokushima-u.ac.jp
[5]Current address: Department of Maxillofacial Orthognathics, Graduate School, Tokyo Medical and Dental University, Tokyo, Japan.
Received 10 October 2007; revised 26 November 2007; accepted 23 January 2008

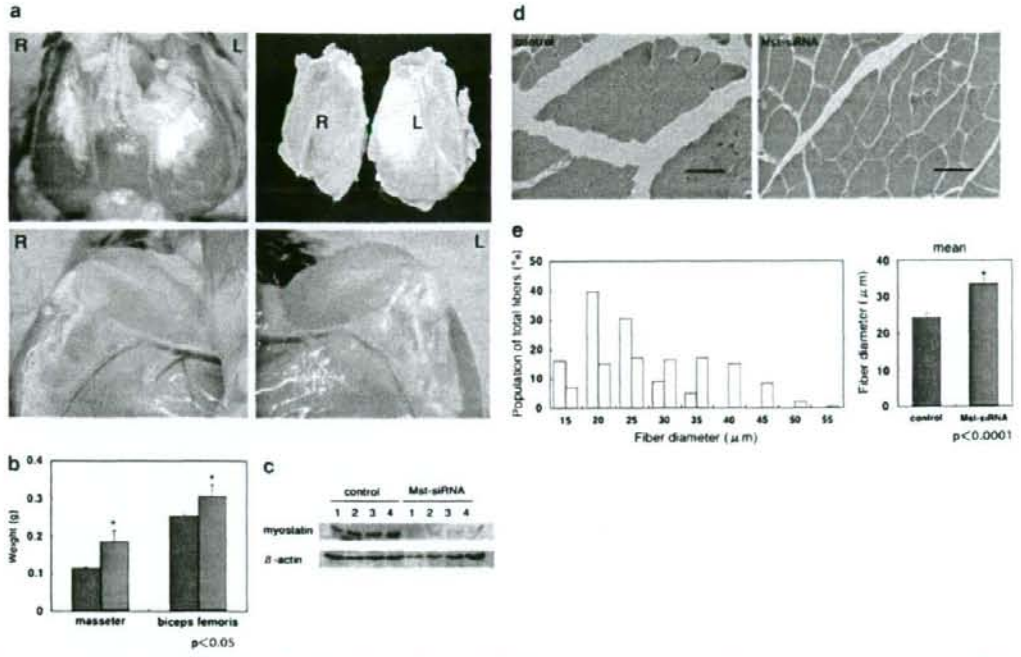

Figure 1 Local administration of the Mst-siRNA/atelocollagen (ATCOL) complex increases skeletal muscle mass and fiber size in wild-type mice through inhibition of myostatin expression. For the experiments depicted in (**a–e**) Mst-siRNAs (final concentration, 10 μM) were mixed with ATCOL (final concentration for local administration, 0.5%.[5]) (AteloGene, Kohken, Tokyo, Japan) according to the manufacturer's instructions. After anesthesia of mice (20-week-old male C57BL/6) by Nembutal (25 mg/kg, i.p.), the Mst-siRNA/ATCOL complex was injected into the masseter and biceps femoris muscles on the left side. As a control, scrambled siRNA/ATCOL complex was injected into the contralateral (right) muscles. After 2 weeks, the muscles on both sides were harvested and processed for analysis. (**a**) Photographs of muscles. Increased muscle mass were observed in the Mst-siRNA/ATCOL-treated (L) masseter (upper panels) and biceps femoris (lower panels), but not in the contralateral muscles (R). (**b**) Muscle weight. Mst-siRNA/ATCOL-treated muscles had an increased weight significantly compared to those with control siRNA/ATCOL (masseter, 0.185 ± 0.041 versus 0.115 ± 0.019 g; biceps, 0.307 ± 0.040 versus 0.232 ± 0.039 g; $n = 4$; $P < 0.05$). Student's *t*-test was used for determining statistical significance. Graphical representation of data uses the following convention: mean ± s.d.; treated muscles or mice in red; control muscles or mice in blue. (**c**) Western blot analysis of myostatin (52 kDa) in the control and Mst-siRNA/ATCOL-treated masseter muscles, assessed at 2 weeks after single injection. Total 80 μg of masseter muscle homogenates were resolved by sodium dodecyl sulfate–polyacrylamide gel electrophoresis and then transferred onto polyvinylidene difluoride membranes for immunoblotting. After a blocking reaction (5% nonfat milk/1% bovine serum albumin in phosphate-buffered saline (PBS) and 0.05% Triton X-100), the blots were incubated for 1 h at room temperature with mouse monoclonal anti-myostatin antibody (1:500; R&D Systems, Minneapolis, MN, USA) or anti-β-actin. After incubation with a secondary antibody (1:10000; horseradish peroxidase-conjugated anti-rat antibody; Biosource International, Camarillo, CA, USA), the blots were developed using the ECL Plus kit (Amersham, Buckinghamshire, UK). We used a purified myostatin protein and proteins extracted from cells transformed with a myostatin cDNA to confirm that the bands are due to 52 kDa myostatin. (**d**) Hematoxylin and eosin staining of the control and Mst-siRNA/ATCOL-treated masseter muscle. Muscles were fixed in 4% paraformaldehyde/PBS at 4 °C overnight, dehydrated and paraffin-embedded. Serial sections (5 μm thickness) were cut at mid-belly of muscle and stained. Scale bar, 50 μm. (**e**) Distribution of myofibril sizes of the control (blue bars) and Mst-siRNA/ATCOL-treated (red bars) muscles. The right panel shows the average myofibril size (33.6 ± 1.5 versus 24.4 ± 1.1 μm; $n = 200$; $P < 0.0001$). NIH Image (NIH, USA) software was used for morphometric measurements.

normalized intracellular myostatin signaling in the model mice for limb-girdle muscular dystrophy 1C.[13] On the other hand, Magee *et al.*[14] demonstrated that downregulation of myostatin expression by transduction of a plasmid expressing a short-hairpin interfering RNA (shRNA) against myostatin using electroporation can increase local skeletal muscle mass. For safety reasons, however, strategies based on vector delivery may be of only limited clinical use. The more desirable approach is to directly apply active siRNAs *in vivo*. As one of the practical platforms for siRNA delivery, we sought to employ an ATCOL-mediated oligonucleotide delivery system to apply myostatin-targeting siRNA into muscles.

We utilized the siRNA sequences reported previously[14] (GDF8 siRNA26, 5′-AAGATGACGATTAT CACGCTA-3′, position 426–446). It has been noted that this sequence can target myostatin mRNA not only of mouse but also human, rat, rabbit, cow, macaque and baboon, based on Blast search (National Center for Biotechnology Information).[14] To confirm the silencing effect of this siRNA, we constructed a plasmid of pSilencer 2.1-U6 neo containing the target sequence and transfected the plasmid into a mouse myoblast cell line, C2C12 cells, which had been made forced to stably express myostatin. We confirmed that the RNAi construct could effectively downregulate the expression

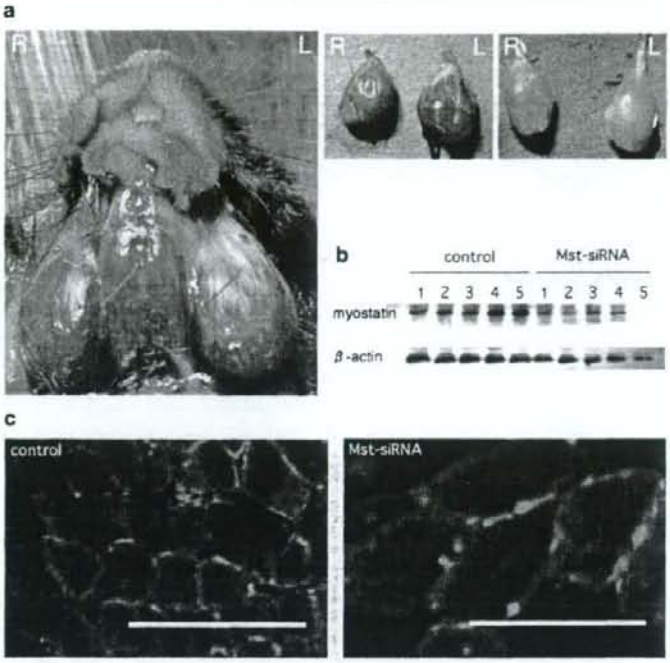

Figure 2 Mst-siRNA/atelocollagen (ATCOL) treatment improves myofibril size in *mdx* mice. (a) Photographs of muscles. The leftward masseter (left and middle panels) and tibial (right panel) muscles injected with the Mst-siRNA/ATCOL complex intramuscularly show a marked increased muscle mass in 20-week-old *mdx* male mice. (b) Western blot analysis of the control and Mst-siRNA/ATCOL-treated masseter muscles, assessed at 2 weeks after single injection. Myostatin protein levels in the muscles injected with the Mst-siRNA/ATCOL complex are markedly decreased, but not in the contralateral muscles injected with the control-siRNA/ATCOL. (c) Immunohistochemical analysis of the cross-sectional myofiber area of the masseter muscle, with the anti-laminin α2 antibody (4H8-2, Sigma, St Louis, MO, USA), showing increased fiber size in the Mst-siRNA/ATCOL-treated (right panel) muscle, compared to that of control (left panel). Alexafluor 594-conjugated anti-rat immunoglobulin G antibodies (A-11007, Invitrogen, Carlsbad, CA, USA) were used for immunohistochemistry. Scale bar, 100 μm.

of myostatin in the C2C12 cells[15] (Supplementary Figure S1).

We prepared the nanoparticle complex containing the GDF8 siRNA26 (10 μM) and ATCOL. Then, we injected the GDF8 siRNA26-ATCOL (Mst-siRNA/ATCOL) complex into the masseter and biceps femoris muscles of 20-week-old C57BL/6 mice. As a control, we injected control-scrambled siRNAs/ATCOL complex in the contralateral muscles. We observed gross morphology of the muscles and dissected the muscle tissues 2 weeks after injection. After injection of the Mst-siRNA/ATCOL complex, both muscles (on the left side) were enlarged, while no significant change was observed on the contralateral side (Figure 1a). We also measured the muscle weight, finding that the Mst-siRNA/ATCOL-treated muscles weighed significantly more than those on the control side (Figure 1b). The Mst-siRNA/ATCOL-treated muscles were further examined by a western blot analysis for myostatin (52 kDa), showing the decreased expression of myostatin on the treated side (Figure 1c). We quantified each result as a ratio to the internal control and statistically analyzed a difference between control (average ratio 0.90 ± 0.07) and treated (average ratio 0.44 ± 0.22) muscles. This difference is significant ($P < 0.01$, Student's *t*-test, $n = 4$). Histological analysis showed that the myofibril sizes of the masseter muscles treated with the Mst-siRNA/ATCOL complex were larger than those of the control (Figure 1d). Examining the sizes of 200 myofibers per group, the population of myofibril sizes indicated a shift from smaller to larger fibers in the Mst-siRNA/ATCOL-treated muscle (Figure 1e). The average myofibril size of the muscle treated with Mst-siRNA/ATCOL gained approximately 1.3 times more than that of control (Figure 1e). No obvious morphological change was observed in other tissues than the treated masseter muscles. In the meanwhile, we did not observe any general sign of ill health and deaths during the period of experiment. These results indicate that the increase of the Mst-siRNA/ATCOL-treated muscle mass is caused by their hypertrophy and that the siRNA complex gives no obvious adverse effects.

We next questioned whether this effect of hypertrophy after local injection of the Mst-siRNA/ATCOL complex observed in normal mice was relevant to dystrophin-deficient *mdx* mouse, an animal model for DMD.[16] We intramuscularly injected the same Mst-siRNA/ATCOL complex into the masseter and tibial muscles on the left side of 20-week-old *mdx* male mice. Within 2 weeks after the single injection, a dramatically increased muscle

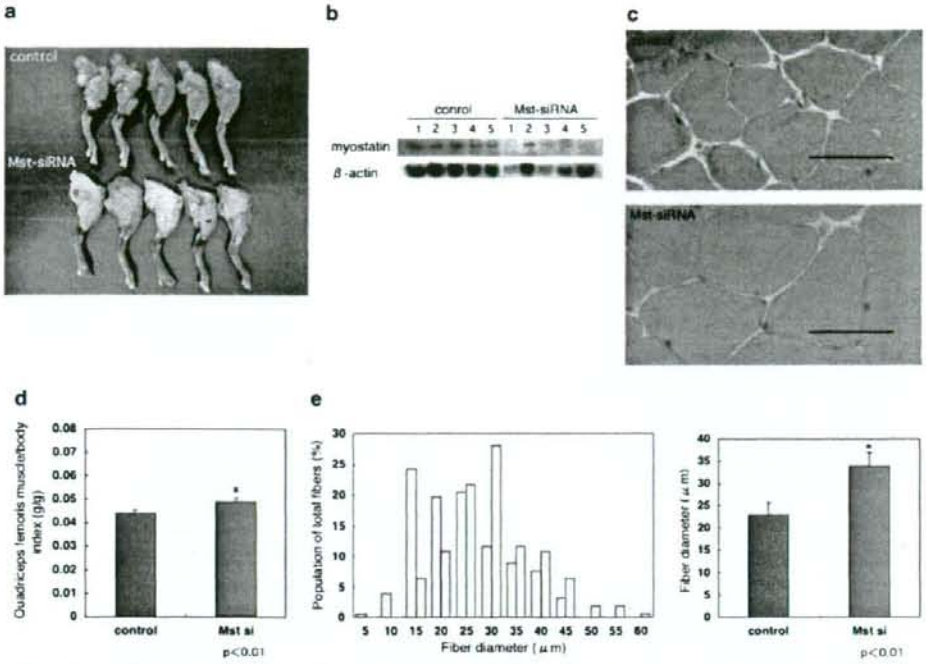

Figure 3 Systemic administration of the Mst-siRNA/atelocollagen (ATCOL) complex induces muscle enlargement in the mouse through inhibition of myostatin expression. For systemic administration, the siRNA (final concentration, 40 μM)/ATCOL (final concentration, 0.05%* complex, 200 μl) was introduced intravenously via orbital veins at 4, 7 and 14 days after the first application ($n=5$). As a control, control-scrambled siRNAs were injected into wild-type male mice (20 weeks, $n=5$). After 3 weeks, the quadriceps muscles on both sides were harvested and processed for analysis. (**a**) Photographs of lower limbs from control (upper panel) and Mst-siRNA/ATCOL-treated (lower panel) mice. (**b**) Western blot analysis of the control and Mst-siRNA/ATCOL-treated muscles (quadriceps femoris), assessed at 3 weeks after triple injection. (**c**) Hematoxylin and eosin staining of the control (upper panel) and Mst-siRNA/ATCOL-treated quadriceps muscle (lower panel). Scale bar, 50 μm. (**d**) Comparison of muscle weight/body weight index between the Mst-siRNA/ATCOL and control-siRNA/ATCOL-treated mice (0.048 ± 0.002 versus 0.043 ± 0.001 $n=5$; $P<0.01$). (**e**) Distribution of myofibril sizes of the control and Mst-siRNA/ATCOL-treated quadriceps muscles. The right panel shows the average myofibril size (33.92 ± 2.91 versus 22.95 ± 1.54 μm, $n=156$; $P<0.01$).

mass was observed in the Mst-siRNA/ATCOL-treated muscle (Figure 2a). Western blot analysis showed that the protein levels of myostatin in the muscles treated with the Mst-siRNA/ATCOL complex were significantly decreased (average ratio 0.55 ± 0.03), but not in the contralateral muscles treated with control siRNAs/ATCOL complex (average ratio 0.83 ± 0.01) (Figure 2b; $P<0.05$, $n=5$). Furthermore, immunohistochemical analysis on the masseter using an anti-laminin α2 antibody showed increase in the mean myofiber size of the Mst-siRNA/ATCOL-treated muscle (Figure 2c), as is the case for the wild-type (not shown). On the basis of these results, it seems that myostatin maintains satellite cells or muscle stem cells in a quiescent state. Reduced myostatin activity would lead to activation of these cells and fusion into existing fibers (Supplementary Figure S1e and f), resulting in fiber hypertrophy as proposed previously.[14]

We further examined whether systemic administration of the Mst-siRNA/ATCOL complex would have an effect on silencing the myostatin expression and lead to muscle enlargement. The Mst- or control siRNA/ATCOL complex was applied intravenously into normal mice four times in 3 weeks. Strikingly, we observed an obvious enlargement of skeletal muscles of lower limbs (Figure 3a), masseters and other muscles. Since change in the muscles of lower limbs is much larger than others, we used them for further analyses. We confirmed reduction of myostatin proteins in the muscles treated with the Mst-siRNA/ATCOL complex (average ratio 0.67 ± 0.11) (Figure 3b; $P<0.01$, $n=5$; average ratio for control 0.87 ± 0.03). We observed that the treated lower limbs are much larger than the controls, although the average body weights were 26.7 ± 0.7 and 25.8 ± 0.4 g for controls and treated mice, respectively. No increase in the body weight of the treated mouse was observed, probably because increase in the muscle weight compensated for reduction of fat accumulation.[17] To show increase in muscle weights, we used the muscle weight/body weight ratio (Figure 3d), in case the body weight exhibited variation. Significant increase in muscle fiber size (Figures 3c and e) was also observed after 3 weeks. These results indicate that siRNAs targeting against myostatin, intravenously administered with ATCOL, can specifically repress the expression of myostatin, inducing muscle hypertrophy in normal mice.

We present evidence that local and systemic applications of siRNA against myostatin coupled with ATCOL markedly stimulate muscle growth *in vivo* within a few

weeks. Local application of siRNA/ATCOL complex was shown to be effective to target the vascular endothelial growth factor gene in a xenografted tumor,[18] while ATCOL was used for systemic siRNA delivery into tumor-bearing mouse models and proved to be effective for silencing exogenous genes as luciferase and metastasis-associated genes as EZH2.[6] However, it has not been elucidated until this study whether the siRNA complex could have an effect of muscle growth on normal tissues by repression of muscle-specific genes. It has been thought that the enhanced permeability and retention (EPR) effect in tumor tissues could facilitate selective targeting of siRNA/polymer complex.[6] In spite of the significance of the EPR effect in tumor therapies, it is noticeable that normal and nontumor diseased tissues can be targets for siRNA-based drugs applied systemically. It was reported that nuclease activity to siRNA could be prevented[18] and cellular uptake of siRNAs was elevated by ATCOL.[5] Although the precise mechanisms by which ATCOL achieves these effects have not been elucidated to date, ATCOL complexed with DNA molecules was demonstrated to be efficiently transduced into mammalian cells.[19] Thus, similarly siRNA/ATCOL complexes may be transduced into cells probably by the same mechanisms as observed for DNA molecules. As a simple administration of myostatin-siRNA/ATCOL complex has a muscle growth effect, this novel method for fighting against muscle atrophy would be of considerable value for clinical applications. In tumor-bearing mice, it was reported that ATCOL could distribute siRNAs against luciferase to normal liver, lung, spleen and kidney tissues as well as bone-metastatic lesions.[6] ATCOL was also reported to display low toxicity and low immunogenicity when it is transplanted *in vivo*.[20,21] Taken together with our results, application of siRNAs with ATCOL would be promising for a therapeutic remedy against various diseases not only of muscles, but also of these organs.

Acknowledgements

We thank Drs Shin-ichiro Nishimatsu, Tsutomu Nohno, Department of Molecular Biology, Kawasaki Medical School for valuable advice. We also thank Shizuka Sasano, Division of Neurology, Kawasaki Medical School and Megumu Kita, Laboratory Animal Center, Kawasaki Medical School for their technical assistances. This work was supported by a Research Grant (14B-4) for Nervous and Mental Disorders from the Ministry of Health, Labour and Welfare; a Grant (15131301) for Research on Psychiatric and Neurological Diseases and Mental Health from the Ministry of Health, Labour and Welfare of Japan and from JSPS KAKENHI (14370212) to SN, YO and YS and by Research Project Grants (15-115B and 16-601) from Kawasaki Medical School to YO and YS.

References

1 Fire A, Xu S, Montgomery MK, Kostas SA, Driver SE, Mello CC. Potent and specific genetic interference by double-stranded RNA in *Caenorhabditis elegans*. *Nature* 1998; **391**: 806–811.

2 Elbashir SM, Harborth J, Lendeckel W, Yalcin A, Weber K, Tuschl T. Duplexes of 21-nucleotide RNAs mediate RNA interference in cultured mammalian cells. *Nature* 2001; **411**: 494–498.

3 de Fougerolles A, Vornlocher HP, Maraganore J, Lieberman J. Interfering with disease: a progress report on siRNA-based therapeutics. *Nat Rev Drug Discov* 2007; **6**: 443–453.

4 Gary DJ, Puri N, Won YY. Polymer-based siRNA delivery: perspectives on the fundamental and phenomenological distinctions from polymer-based DNA delivery. *J Control Release* 2007; **121**: 64–73.

5 Minakuchi Y, Takeshita F, Kosaka N, Sasaki H, Yamamoto Y, Kouno M *et al*. Atelocollagen-mediated synthetic small interfering RNA delivery for effective gene silencing *in vitro* and *in vivo*. *Nucleic Acids Res* 2004; **32**: e109.

6 Takeshita F, Minakuchi Y, Nagahara S, Honma K, Sasaki H, Hirai K *et al*. Efficient delivery of small interfering RNA to bone-metastatic tumors by using atelocollagen *in vivo*. *Proc Natl Acad Sci USA* 2005; **102**: 12177–12182.

7 Takeshita F, Ochiya T. Therapeutic potential of RNA interference against cancer. *Cancer Sci* 2006; **97**: 689–696.

8 McPherron AC, Lawler AM, Lee SJ. Regulation of skeletal muscle mass in mice by a new TGF-beta superfamily member. *Nature* 1997; **387**: 83–90.

9 Deconinck N, Dan B. Pathophysiology of Duchenne muscular dystrophy: current hypotheses. *Pediatr Neurol* 2007; **36**: 1–7.

10 Foster K, Foster H, Dickson JG. Gene therapy progress and prospects: Duchenne muscular dystrophy. *Gene Therapy* 2006; **13**: 1677–1685.

11 Bogdanovich S, Krag TO, Barton ER, Morris LD, Whittemore LA, Ahima RS *et al*. Functional improvement of dystrophic muscle by myostatin blockade. *Nature* 2002; **420**: 418–421.

12 Nishi M, Yasue A, Nishimatsu S, Nohno T, Yamaoka T, Itakura M *et al*. A missense mutant myostatin causes hyperplasia without hypertrophy in the mouse muscle. *Biochem Biophys Res Commun* 2002; **293**: 247–251.

13 Ohsawa Y, Hagiwara H, Nakatani M, Yasue A, Moriyama K, Murakami T *et al*. Muscular atrophy of caveolin-3-deficient mice is rescued by myostatin inhibition. *J Clin Invest* 2006; **116**: 2924–2934.

14 Magee TR, Artaza JN, Ferrini MG, Vernet D, Zuniga FI, Cantini L *et al*. Myostatin short interfering hairpin RNA gene transfer increases skeletal muscle mass. *J Gene Med* 2006; **8**: 1171–1181.

15 Artaza JN, Bhasin S, Magee TR, Reisz-Porszasz S, Shen R, Groome NP *et al*. Myostatin inhibits myogenesis and promotes adipogenesis in C3H 10T(1/2) mesenchymal multipotent cells. *Endocrinology* 2005; **146**: 3547–3557.

16 Bulfield G, Siller WG, Wight PA, Moore KJ. X chromosome-linked muscular dystrophy (mdx) in the mouse. *Proc Natl Acad Sci USA* 1984; **81**: 1189–1192.

17 McPherron AC, Lee SJ. Suppression of body fat accumulation in myostatin-deficient mice. *J Clin Invest* 2002; **109**: 595–601.

18 Takei Y, Kadomatsu K, Yuzawa Y, Matsuo S, Muramatsu T. A small interfering RNA targeting vascular endothelial growth factor as cancer therapeutics. *Cancer Res* 2004; **64**: 3365–3370.

19 Honma K, Ochiya T, Nagahara S, Sano A, Yamamoto H, Hirai K *et al*. Atelocollagen-based gene transfer in cells allows high-throughput screening of gene functions. *Biochem Biophys Res Commun* 2001; **289**: 1075–1081.

20 Ochiya T, Nagahara S, Sano A, Itoh H, Terada M. Biomaterials for gene delivery: atelocollagen-mediated controlled release of molecular medicines. *Curr Gene Ther* 2001; **1**: 31–52.

21 Sano A, Maeda M, Nagahara S, Ochiya T, Honma K, Itoh H *et al*. Atelocollagen for protein and gene delivery. *Adv Drug Deliv Rev* 2003; **55**: 1651–1677.

Supplementary Information accompanies the paper on Gene Therapy website (http://www.nature.com/gt)

Acta Myologica • 2008; XXVII; p. 30-36

Vasodilation of intramuscular arterioles under shear stress in dystrophin-deficient skeletal muscle is impaired through decreased nNOS expression

K. Sato[1, 2, 3], T. Yokota[1], S. Ichioka[4], M. Shibata[5], S. Takeda[1]

[1] *Department of Molecular Therapy, National Institute of Neuroscience, National Center of Neurology and Psychiatry, Kodaira, Tokyo 187-8502, Japan;* [2] *Cellport Clinic Yokohama, Minami-nakadori 3-35, Naka-ku, Yokohama, Kanagawa, 231-0006, Japan;* [3] *Department of Plastic and Reconstructive Surgery, Graduate School of Medicine, The University of Tokyo, Bunkyo-ku, Tokyo 113-0033, Japan;* [4] *Department of Plastic and Reconstructive Surgery, Saitama Medical School, Moroyama, Iruma-gun, Saitama 350-0451, Japan;* [5] *Department of Biomedical Engineering, Graduate School of Medicine, The University of Tokyo, Bunkyo-ku, Tokyo 113-0033, Japan*

Duchenne muscular dystrophy (DMD) is a lethal X-linked disorder of striated muscle caused by the absence of dystrophin. Recently, impairment of vascular dilation under shear stress has been found in DMD, but the underlying molecular mechanism is not fully understood. Moreover, dilation of intramuscular arterioles, which may be a key to the molecular pathogenesis, has not been addressed yet. We examined dilation of arterioles in the mouse cremaster muscle under shear stress due to ligation. The vasodilation was significantly impaired in dystrophin-deficient *mdx* mice as well as in neuronal nitric oxide synthase (nNOS)-deficient mice; however, neither endothelial NOS-deficient mice nor α1-syntrophin-deficient mice showed any difference in vasodilation from control mice. These results indicate that nNOS is the main supplier of nitric oxide in shear stress-induced vasodilation in skeletal muscle, but that the sarcolemmal localization of nNOS is not indispensable for the function. In contrast, the response to acetylcholine or sodium nitroprusside was not impaired in *mdx* or nNOS-deficient mice, suggesting that pharmacological treatment using a vasoactive agent may ameliorate skeletal and cardiac muscle symptoms of DMD.

Key words: Duchenne muscular dystrophy, blood flow, dystrophin, nitric oxide synthase, vasodilation

Introduction

Nitric oxide (NO) is a vasoactive agent generated by nitric oxide synthase (NOS). Neuronal NOS (nNOS) is highly expressed in skeletal muscle compared with endothelial NOS (eNOS) and inducible NOS (iNOS). nNOS is anchored by α1-syntrophin, a member of the dystrophin-glycoprotein complex (DGC), at the sarcolemma in skeletal muscle (1-6). Dystrophin is a cytoskeletal protein, and its absence together with the secondary loss of DGC from the sarcolemma is responsible for Duchenne muscular dystrophy (DMD), a severe muscle disease characterized by progressive skeletal muscle degeneration complicated with cardiomyopathy (5). nNOS expression is greatly reduced at the mRNA level in dystrophin-deficient muscle (2). Moreover, the attenuation of α-adrenergic vasoconstriction is impaired in contracting dystrophin-deficient muscle, suggesting that nNOS has a specific role in protection from sympathetic vasoconstriction (7, 8). In addition, the localization of nNOS at the sarcolemma through α1-syntrophin is indispensable for the attenuation of α-adrenergic vasoconstriction during muscle contraction (9). Recently, Loufrani et al. showed that the carotid and mesenteric arteries of *mdx* mice, an animal model of DMD, do not dilate properly under shear stress, although they are dilated normally by treatment with either an NOS stimulator, such as acetylcholine (ACh), or an NO donor, such as sodium nitroprusside (SNP) (10). They concluded that the endothelial dystrophin plays an invaluable role in vasodilation under shear stress. In addition, the molecular background is not clearly understood, although flow-induced remodeling in arterial wall is deficient in *mdx* mice when stimulated by arterial ligation or hydralazine (11, 12). To clarify the role of nNOS in intramuscular arterioles in vivo, we studied vasodilation in the mouse cremaster muscle. We caused the modified parallel occlusion of arterioles by microsurgical nylon thread ligation (13-16). We enlisted the participation of DGC in shear-stress vasodilation by using *mdx* mice. We also determined the significance of the localization of nNOS at the sarcolemma by using α1-

Address for correspondence: S. Takeda, Department of Molecular Therapy, National Institute of Neuroscience, National Center of Neurology and Psychiatry, 4-1-1 Ogawa-higashi, Kodaira, Tokyo 187-8502, Japan. Fax +81 42 3461750. E-mail: takeda@ncnp.go.jp